Spatially explicit Bayesian hierarchical models for avian population status and trends

Adam C. Smith[1*], Allison Binley[2], Lindsay Daly[1], Brandon P.M. Edwards[1,2], Danielle Ethier[3], Barbara Frei[4], David Iles[1], Timothy D. Meehan[5], Nicole L. Michel[5], Paul A. Smith[6]

1 Canadian Wildlife Service, Environment Climate Change Canada, Ottawa Canada.

2 Carleton University, Department of Biology, Ottawa Canada..

3 Birds Canada, Port Rowan, Ontario N0E 1M0, Canada

4 Wildlife Research – East, Environment Climate Change Canada, Québec Canada.

5 National Audubon Society, 225 Varick Street, New York, NY 10014 USA.

6 Wildlife Research Division, Environment Climate Change Canada, Ottawa Canada.

*Corresponding Author: adam.smith@ec.gc.ca

ACKNOWLEDGEMENTS

We sincerely thank the volunteers from all three surveys; the thousands of U.S. and Canadian participants who annually conduct and coordinate the North American Breeding Bird Survey, the thousands who participate in the Audubon Christmas Bird Count and the MSS volunteers who contributed their time, in some cases over a period of decades. CBC Data are provided by National Audubon Society and through the generous efforts of Bird Studies Canada and countless volunteers across the Western Hemisphere. For the MSS, support and coordination of the surveys were provided by Environment and Climate Change Canada and Manomet Inc., with additional significant contributions from the United States Fish and Wildlife Service. There are no known conflicts of interest.

DATA AVAILABILITY

The Breeding Bird Survey data is available online (U.S. Geological Survey and Canadian Wildlife Services 2021), Migratory Shorebird Survey data are freely available via NatureCounts (Birds Canada 2023) and eBird data can be accessed through their website (eBIRD 2022), and the Audubon Christmas Bird Count is available through their website as well (Audubon 2022). Code archive is available on GitHub for review (Smith 2023) and will be archived online when published. All BBS analyses can be replicated using bbsBayes2 in R (Edwards et al. 2023).

ABSTRACT

Population trend estimates form the core of avian conservation assessments in North America and indicate important changes in the state of the natural world. The models used to estimate these trends would be more efficient and informative for conservation if they explicitly considered the spatial locations of the monitoring data. We created spatially explicit versions of some standard status and trend models applied to long-term monitoring data for birds across North America. We compared the spatial models to simpler non-spatial versions of the same models, fitting them to simulated data and real data from three broad-scale monitoring programs: the North American Breeding Bird Survey (BBS), the Christmas Bird Count (CBC), and a collection of programs we refer to as Migrating Shorebird Surveys (MSS). All the models generally reproduced the true simulated trends and population trajectories when there were many data, but the spatial models outperformed the non-spatial models when there were fewer data and in locations where the local trends differed from the range-wide means. When fit to real data, the spatial models revealed interesting spatial patterns in trends that were much less apparent in results from the non-spatial versions. The spatially explicit sharing of information also means we can fit the models with much smaller strata, allowing for finer-grained patterns in trends. Spatially informed trends will facilitate more locally relevant conservation, highlight areas of conservation successes and challenges, and help generate and test hypotheses about the spatially dependent drivers of population change.

Keywords: abundance, Bayesian, GAM, hierarchical, iCAR, biological monitoring, spatially explicit

LAY SUMMARY

- We created population trend models that share information on species abundance and trend among neighboring regions and compared those to models without spatial information
- Trends and population trajectories through time were more accurate and precise with the spatial models than models without the spatial information
- The predictions from these models (trends, trajectories, maps of patterns in trends, etc.) will improve our understanding of the status of bird populations in time and space, and guide future research into the drivers of ongoing avian population declines.

INTRODUCTION

The status of wildlife populations is often reported at range-wide spatial scales (IUCN 2001, Rosenberg et al. 2019, van Klink et al. 2020), however, the fine-scale estimates produced by spatial models are biologically-relevant, robust and necessary for local conservation actions. Factors that affect wildlife populations are often spatially structured, such as habitat change, human activity, (Hill et al. 2014, Stanton et al. 2018) precipitation, temperature, and phenology (Renfrew et al. 2013, Wilson et al. 2018). For migratory birds, varying conditions through the annual cycle can lead to complex spatial patterns in population change (Morrison et al. 2010, 2013). Populations with strong migratory connectivity can exhibit similar trends among neighboring populations in the breeding and nonbreeding seasons (Michel et al. 2016, 2021; Koenig and Liebhold 2016), while spatial patterns in trends can be obscured when populations mix during one or more phases of the annual cycle (Finch et al. 2017). Addressing this spatial complexity through appropriate modeling choices should produce estimates that are more accurate at all spatial scales, and, at the finer spatial scales that are most relevant for directing conservation action. For example, modeling frameworks that share information among neighboring regions allow for more robust estimates in data-sparse areas, strengthen inference by reducing spatial autocorrelation in model residuals, and allow for the finer-scale estimates of abundance and trend that are critical for conservation decision-making.

Hierarchical models commonly used to assess patterns in avian population dynamics share information across the entire species' range by shrinking estimates in each region towards a global mean (Soykan et al. 2016, Meehan et al. 2019, Smith and Edwards 2020). For example, hierarchical generalized additive models (GAMs) can track non-linear population change (Fewster et al. 2000, Pedersen et al. 2019), and the parametric components of the smooths can share information in space on the shape of the population trajectory (Smith and Edwards 2020). This class of models fits a smooth relationship between a vector of predictor variables and a response variable using semi-parametric spline smoothers, while allowing for partial pooling of the smooths among groups (Wood 2017, Pedersen et al. 2019). In ecology, hierarchical GAMs have been used for a variety of contexts and systems, including tracking shifts in spatial regimes of birds in the Great Plains (Roberts et al. 2022), exploring abundance patterns in mountain bumble bees (Sponsler et al. 2022), integrating multiple data sources and survey types in sea animal surveys (Miller et al. 2021), and estimating smooth population trend trajectories of North American breeding birds (Smith and Edwards 2020). Although the parameters of a spline smooth are not directly interpretable as "population change", for a given basis function, each of the parameters defines a consistent relationship between the data, the predictor (time), and the model predictions (estimates of relative abundance through time). Treating the parameters of a spline smooth as random terms in a hierarchical model is like treating the parameters for other predictors as random terms that vary among strata. In this case, the inference is based only on the combined effect of all predictors in the matrix (i.e., the predicted smooth temporal pattern), instead of the independent effects of each predictor.

Similarly, the first-difference model for the BBS (Link et al. 2017) could also share information on parameters that represents population change. This first-difference model as applied to date (Link et al. 2020), does not share information among regions, instead, it estimates a population trajectory using a first-order, auto-regressive random walk. However, this same model could be re-parameterized as a series of annual differences, where estimates of the difference between years in a given stratum are informed by the mean difference across the species' range in that year or the mean of the same annual differences in neighboring regions. Parameterized this way, the annual differences can share information across the full species' range to pool estimates towards a global annual mean, or in a spatially explicit way to pool estimates towards a local mean.

Intrinsic Conditional Autoregressive (iCAR) structures provide a practical approach to implementing the spatially explicit sharing of information in models of wildlife trends (Ver Hoef et al. 2018, Morris et al. 2019). iCAR models include a parameter that estimates the amount of variation among neighboring strata, where strata are defined as neighbors based on a sparse matrix of spatial adjacencies (Besag et al. 1991). Spatial iCAR structures have been used to model the annual abundance of birds in Breeding Bird Survey (BBS) data (Bled et al. 2013).

However, this earlier BBS model did not explicitly model the rate of population change as a parameter in the model. Instead, it shared information in space but not in time, modeling spatially explicit but temporally independent estimates of annual abundance, and trends were a summary of annual values of predicted abundance. iCAR structures have also been used to model fine-scale population trends in Christmas Bird Count (CBC) data (Meehan et al. 2019). For the CBC models, trends were modeled as a single parameter (i.e., a log-linear slope parameter) that assumed some constant rate of change in each location over time (Meehan et al. 2019). Spatially explicit, versions of the non-linear GAM and first-difference models expand upon these earlier models, by allowing for more complex temporal trajectories that can track variations in trends through time and space.

Goal

We describe models with simple hierarchical structures that shrink estimates towards a global mean (herein, ‘non-spatial’ models) and models with spatially explicit iCAR structures that shrink estimates towards a local mean by sharing information among neighboring strata (herein, spatial model). The non-spatial and spatial models were applied to the Generalized Additive Model with Year Effects (“GAMYE”) used by the Canadian Wildlife Service (CWS; Smith and Edwards 2020) and the first-difference model used by the United States Geological Survey (USGS; Link et al. 2020). The GAMYE and first-difference models provide relevant examples of the benefits of sharing information among regions on the parameters of interest in a status and trend assessment of birds in North America. We fit models to simulated data and then applied to examples of real data from three long-term bird monitoring programs. Real data came from the North American Breeding Bird Survey (BBS; Ziolkowski Jr. et al. 2022), the Audubon

Christmas Bird Count (CBC; Soykan et al. 2016), and the Migrating Shorebird Survey (MSS; Howe et al. 1989, Morrison et al. 1994, Ross et al. 2012). By explicitly accounting for the spatial relationships among the data, our goal is to develop trend models that can inform conservation decision-making at multiple spatial scales by 1) producing estimates at finer spatial resolutions, 2) producing better estimates for data-sparse regions and 3) providing a widely applicable statistical framework for any species or standardized monitoring programs.

METHODS

The following subsections outline the modeling techniques used in this study and describe the metrics used to estimate population trends. We start by introducing the general underlying structure of the models for population change. Then, we describe the spatial iCAR structure that we used for the spatial models, including details about derivations of neighborhood relationships. We then describe in detail, the temporal components of two models for population change: the generalized additive model with year effects (GAMYE), and the first difference model. By modeling changes in counts through time, we produced estimates of population trajectories and trends, which we describe in detail. Finally, we finish this section by describing assessments of model performance, including estimation accuracy with a simulated data set and application of the models to real monitoring data from the three long-term monitoring programs.

Model Structure

The models here are based on a consistent underlying structure, with variations to the components that model the temporal change (e.g., annual differences or temporal smooths) and variations to compare spatial and non-spatial versions. Additionally, we included variations to account for the specifics of the three real datasets used in the examples. All the data, models, and code needed to fit these models are provided in the supplements (for review purposes: https://github.com/AdamCSmithCWS/Spatial_Hierarchical_Trend_Models [will be permanently archived on Zenodo when published]).

The models all rely on survey counts of a given species ($C_{j,i,t}$), conducted at site-j, in stratum-i, during year-t, as realizations of a negative binomial distribution, with mean $\lambda_{j,i,t}$ and inverse dispersion parameter ϕ. On the log scale, the values of λ were modeled by intercepts representing the mean counts for each stratum (α_i) and observation site (ψ_j), plus a temporal component that estimates the population trajectory through time (i.e., annual values of relative abundance $\Delta_{i,t}$).

$$C_{j,i,t} = Negative\ Binomial\left(\lambda_{j,i,t}, \phi\right)$$

$$log\left(\lambda_{j,i,t}\right) = \alpha_i + \psi_j + \Delta_{i,t}$$

We estimated the site intercepts as partially pooled parameters that shared information among all sites in the species' dataset ($\psi_j \sim N\left(0,\ \sigma_\psi^2\right)$). We also estimated the stratum intercepts (α_i) and population trajectories ($\Delta_{i,t}$) as partially pooled parameters, sharing information among all strata, however, the specific hierarchical structures vary among the models and between spatial and non-spatial versions of each model. For each of the real and simulated datasets used here (BBS, CBC, and MMS), the models required modifications to accommodate the idiosyncrasies of each survey. Briefly (more detail in the supplemental materials), the BBS model has two extra observer-effects to account for both among and within observer variation; the CBC model has an extra effort-correction to account for the varying number of observers and time spent observing;

and the MMS model has an extra smooth to account for variable abundance throughout the migration season and simplified treatment of the year-effects.

Spatial iCAR

The spatial versions of our models used an intrinsic conditional autoregressive approach (Besag et al. 1991). This iCAR spatial structure shares information among strata using a connected network graph of adjacent strata, where values in each stratum (i) are most similar to those in the collection of N_i neighboring spatial strata (Figure 1). The intercepts modeling the log-scale mean counts within a given stratum provide a general example of how the iCAR structures incorporate spatial information in estimating local parameters. The stratum intercepts (α_i) are an additive combination of an overall hyperparameter mean and a stratum-specific component ($\alpha_i = \alpha' + \alpha_i''$). In each stratum-i, the stratum-specific component (α_i''), is drawn from a normal distribution, centered on the mean of the same parameter in all neighboring strata and with standard deviation estimated across all strata and scaled by the inverse of the number of neighbors. The standard deviation term estimates the degree of spatial smoothing for the parameter. We conducted prior predictive simulations to define weakly informative priors on the spatial variance of the temporal parameters in our models (supplemental information)

$$\alpha_i'' \sim Normal\left(\frac{\sum_{n \in N_i} \alpha_n''}{N_i}, \frac{\sigma_{\alpha''}}{N_i}\right)$$

We used Stan language functions and methods defined in (Morris et al. 2019) to estimate the spatial iCAR component.

We grouped long-term survey sites into geographic strata to allow the model to estimate varying population trajectories across the continent, while sharing information among sites in relatively close proximity (Figure 1). For the BBS and CBC data, we used the same strata used in recent analyses of these data (following: Sauer and Link 2011, Soykan et al. 2016, Smith and Edwards 2020), where the strata are defined by intersections of state and provincial boundaries with Bird Conservation Regions (North American Bird Conservation Initiative U.S. Committee 2000). For the shorebird data, we grouped individual survey sites within a regular hexagonal grid, with grid cells approximately 300 km in diameter. For the simulated data here, we used the BBS strata with data for the Pine Warbler (*Setophaga pinus*): a species with a relatively broad geographical distribution across the eastern portion of the continent.

We defined the neighborhood relationships among the strata based on shared edges of the strata polygons (Figure 1). For a species with s-strata, the s*s adjacency matrix has a value of 1 in all cells that share an edge and 0 in all other cells. For one of the real datasets used here (MSS), not all strata had adjacent neighbors (i.e., data were missing from some intervening strata). To ensure that the adjacency matrix would be fully connected in this case, we defined the spatial neighborhood relationships using a Voronoi tessellation of the centers of the strata that contributed data to the analysis. This Voronoi tessellation approach partly distorts the spatial relationships among strata, because it considers some strata neighbors even though they are separated by much larger distances than other neighboring strata. The ideal approach to modeling spatial areal data with disconnected graphs is an open area of research (Freni-Sterrantino et al. 2018). For example, one could retain enough of the intervening strata in the graph to retain the spatial relationships and fully connect the graph, while supplying the model with no data for these regions (Meehan et al. 2019), and increasing the computational needs of the model. The simplification we have used here approximates the relative spatial relationships, if not the absolute spatial relationships, and allows the model to shrink estimates in these isolated strata towards estimates in the next nearest strata (Smith et al. 2014), without requiring the estimation of many additional parameters that are not informed by data.

Models for Population Change

Here we focus on two approaches to modeling non-linear temporal change in populations, a non-linear smooth with added year-effects (“GAMYE”) and a model that estimates the first-order differences between subsequent years (“first-difference”). These two approaches are examples of hierarchical Bayesian approaches that have been used to model the temporal component of long-term monitoring programs, and which have been fully described in previous work (Link and Sauer 2002, Soykan et al. 2016, Link et al. 2020, Smith and Edwards 2020). The various published approaches model the time series using some combination of first-order differences, linear slopes with random year-effects, or non-linear smooths with or without random year-effects (Smith and Edwards 2020). For application to the BBS data, these published models can be accessed through the R packages bbsBayes2 (Edwards et al. 2023), and bbsBayes (Edwards and Smith 2021).

GAMYE. The GAMYE model uses semi-parametric smooths (the “GAM” component) plus random annual fluctuations (i.e., “year effects” that make up the “YE” component) around the smooths to model the population trajectories (Smith and Edwards 2020). We estimated the smooths as a hierarchical generalized additive model (HGAM) with a global mean-smooth hyperparameter and stratum-level smooths that describe local deviations from the global mean. The model used here is like the model in (Smith and Edwards 2020), but with an alternative spline basis and a modified hierarchical structure that improves model performance. The smooth trajectories in each stratum (δ_i) are an additive combination of the K-length vector of coefficients B_i multiplied by the basis function matrix for the spline (X) that has one row for each year and K-columns (1 for each of the K-knots of the basis).

$$\delta_i = X * B_i$$

The coefficients (B_i) are an additive combination of hyperparameter means and stratum-level parameters $B_i = B' + B''_i$. Since the basis matrix (X) is a fixed matrix of data, this is mathematically equivalent to an additive combination of a mean hyperparameter smooth ($\delta' = X * B'$) and a stratum-specific smooth ($\delta''_i = X * B''_i$).

$$\delta_i = \delta' + \delta''_i$$

The key difference between the non-spatial and spatial versions of the GAMYE is the way the B''_i parameters share information. In the non-spatial version, the stratum-level parameters share information within each stratum, across the k-parameters (Wood 2017, Pedersen et al. 2019). They are mean-zero varying effects $B''_i \sim Normal(0, \sigma_{B''_i})$, shrunk towards 0 in each stratum. In the spatial version, the stratum level parameters for each knot in the spline share information among strata (i.e., spatially), and are shrunk towards the mean values in neighboring strata. This spatially explicit sharing of information assumes values of the GAM coefficients in each stratum (i) are most similar to those in the collection of N_i neighboring spatial strata.

$$\beta''_{i,k} \sim Normal\left(\frac{\sum_{n \in \mathrm{N}_i} \beta''_{n,k}}{N_i}, \frac{\sigma_{B''_k}}{N_i}\right)$$

We used low-rank, thin-plate regression splines (Wood 2017), a different basis than the one used in (Smith and Edwards 2020). We also scaled the basis to include sum-to-zero identifiability constraints to improve the sampling performance. This basis and constraints are the default basis used in the Bayesian R-packages brms (Bürkner 2017) and rstanarm (Gabry and Goodrich n.d.). The design matrix was generated in R and entered the model as data. We set K (the number of knots and a control on the maximum complexity of the smooth) to approximately 1 knot for every 4 years in the dataset, following Smith and Edwards (2020). This value of K controls the upper limit on the complexity of the smooth and is a balance between allowing the smooth to track the short- and medium-term population fluctuations that are similar among strata, while helping the model separately estimate the smooth component from the year effects. The annual fluctuations ($\gamma_{i,t} \sim N(0, \sigma_{\gamma_i})$) were estimated as stratum-specific, zero-mean random departures from the smooths, with a stratum-specific estimated standard deviation (σ_{γ_i}). The full temporal component of the trajectory is the sum of the smooth component and the year effects.

$$\Delta_{i,t} = \delta_{i,t} + \gamma_{i,t}$$

First-Difference. We based our first-difference models on the one originally described (Link et al. 2017), but with a hierarchical modeling approach. In our models, information is shared among strata across the species' range, instead of independently estimating the population trajectories in each stratum. In this first-difference model, we fixed the temporal components for each stratum at 0 for the year in the middle of the time-series ($\Delta_{i,t_{fixed}} = \pi_{i,t_{fixed}} = 0$), to ensure the intercepts and differences are estimable, following (Link et al. 2017). In the latter half of the time-series, the temporal component in stratum-i and year-t is the sum of its value in the previous year ($\Delta_{i,t-1}$) and a difference value ($\pi_{i,t}$), which is itself a sum of a mean hyperparameter difference for year-t (π'_t) and a stratum-specific difference ($\pi''_{i,t}$).

$$\Delta_{i,t} = \Delta_{i,t-1} + \pi_{i,t}$$

$$\pi_{i,t} = \pi'_t + \pi''_{i,t}$$

In the first half of the time-series, the differencing works backwards in time, so that the temporal components in year-t are its value in the following year minus a difference value ($\Delta_{i,t} = \Delta_{i,t+1} - \pi_{i,t}$). We estimated the stratum-specific values of annual differences as zero-mean, random deviations from the survey-wide hyperparameter mean $\pi''_{i,t} \sim normal(0, \sigma_{\pi''})$.

In the spatial versions of the model, we estimated the stratum-specific values of annual differences using the spatial iCAR structures.

$$\pi''_{i,t} \sim Normal\left(\frac{\sum_{n \in \mathrm{N}_i} \pi''_{i,t}}{N_i}, \frac{\sigma_{\pi''}}{N_i}\right)$$

For both the spatial and non-spatial versions of the first-difference model, we used zero-sum constraints in each year to ensure the stratum-level differences were centered on the hyperparameter difference value.

Population Trajectories

The estimated population trajectories for each stratum were defined by the collection of estimated annual indices of abundance ($n_{i,t}$). These annual indices were calculated as the exponentiated sums of the temporal components and the stratum and site intercepts. We kept the terms for all of the seasonal, observer, or effort parameters at 0. Following (Smith and Edwards 2020), we accounted for the variance in annual indices in abundance (herein abundance) among sites by generating predictions for the set of sites-j included in stratum-i, ($j \in S_i$) then averaging the predicted values across those sites.

$$n_{i,t} = \frac{\sum_{j \in S_i} e^{\alpha_i + \psi_j + \Delta_{i,t}}}{S_i}$$

We also calculated smoothed population trajectories for the GAMYE, as above but without the parameter for annual fluctuations. These smoothed stratum-level population trajectories provide an estimate of the medium and long-term patterns of population change after removing the effects of the random annual fluctuations and form the basis of our trend calculations.

$$nSmooth_{i,t} = \frac{\sum_{j \in S_i} e^{\alpha_i + \psi_j + \delta_{i,t}}}{S_i}$$

For surveys where the relative counts of birds can be meaningfully compared among strata (e.g., BBS or CBC surveys where effort is controlled or adjusted for in the model), population trajectories for composite regions (all strata, or a collection of strata included in a country) were calculated following (Soykan et al. 2016, Smith and Edwards 2020) and other models for the BBS and CBC data. Briefly, these composite regions are means of the stratum-level trajectories, where the means are weighted by the area of the strata and the proportion of sites in each stratum that were included in the model for a given species. For the MSS surveys where the relative counts of birds cannot be meaningfully compared (Smith et al. 2023), the survey-wide population trajectory was estimated using the mean smoothed trajectory, the hyperparameter for the abundance intercept, and adding a variance component for the site effects.

$$NSmooth_t = e^{\alpha' + \Delta_t + \sigma_\psi^2 * 0.5 + \sigma_\gamma^2 * 0.5}$$

Trends

Multiple metrics can be used to estimate a “trend” from an estimated population trajectory (see discussions in (Sauer and Link 2011, Smith and Edwards 2020). Here we have used “end-point” trends that estimate the geometric mean annual changes (%/year) in the population trajectories, using interval-specific ratios of annual indices at the start and end years of a time-period. As a specific example, these end-point trends from year t_a to year t_b for the population in a given stratum was:

$$Trend_{t_a,t_b} = 100 * \left(\left(\frac{n_{i,t_b}}{n_{i,t_a}} \right)^{\frac{1}{t_b - t_a}} - 1 \right).$$

A similar end-point trend can be calculated using the smoothed population trajectory from the GAMYE model by replacing $n_{i,t}$ with $nSmooth_{i,t}$ in the trend equation, following (Smith and Edwards 2020), and herein "smooth end-point" trends. Unless otherwise indicated, trends from the first difference models are always end-point trends as defined above, and trends for the GAMYE models are always smooth end-point trends.

Simulated Data

To demonstrate and compare the models, we simulated counts from a broad-scale annual monitoring program like the BBS for a 56-year time-series. We simulated annual counts on BBS routes using the real spatial and temporal structures of the data for Pine Warbler to provide the spatial relationships among strata, routes, observers, and survey schedules (the annual schedule of routes surveyed, active observers, and turn-over in observers through time). We simulated annual counts with a relatively simple spatial pattern in mean abundance and non-linear long-term patterns of population change that varied depending on the latitude of the strata. The mean abundance of our simulated species peaked at the mid-latitudes of its distribution, and the long-term population trends were most negative in the North and most positive in the South. We simulated an overall population trajectory for each region that was a combination of a long-term trend, a non-linear pattern based on annual values of a climatological cycle, and stratum-specific random annual fluctuations. We simulated three datasets that were identical except for the simulated species mean counts, to contrast how the model performs with different levels of information. The simulated mean counts for the three datasets were 0.1, 1.0, and 10 birds observed per year on an average BBS route. The specific patterns in the true underlying population trajectories are not particularly important for the model comparisons here, but they were designed to reflect a species population trajectory that showed geographic variation in both abundance and changes in abundance that are strong but biologically plausible: additive effects of long-term trends with a cycle and annual fluctuations (Wilson et al. 2018).

We simulated the temporal patterns in population change using a long-term trend that varied by latitude (stable in the south and increasing in the north). The cyclic component was simulated as a local response to a smooth of the Pacific Decadal Oscillation (PDO; Albers 2022), where the magnitude of the response to the PDO varied by latitude so that it was strongest in the northern part of the species' range and almost non-existent at the southern edge. We also added local annual fluctuations based on annual values of the PDO, but these annual components were constant across the species' range (i.e., did not vary in space). We set the mean abundance for each stratum using a similar deterministic component based on the latitude of each stratum, so that the species' mean observed counts would be highest in strata closest to the latitudinal mid-point of the species' range. To this true underlying population trajectory (including the mean abundance, long-term trend, smooth cyclic component, and deterministic annual fluctuations), we added some random annual fluctuations within each stratum, random variation in mean abundance among routes and mean counts by observers, as well as count-level random noise.

The exponent of the sum of all these true effects provided the expected value of a Poisson distribution, and realizations from those distributions were the simulated counts used as data in the models. In summary, the simulated data represented reasonable observed counts from a program like the BBS, with a known geographic pattern of non-linear population change with long-term, medium-term, and short-term variation. For more information and our simulation code, see the supplementary materials.

Comparisons of Estimation Accuracy

We fit the spatial and non-spatial versions of the models to these simulated data and compared the estimation accuracy of the two approaches. We assessed how well the models were able to reproduce the true patterns of population change in each stratum by visual comparisons of the estimated and true trajectories. We also compared the accuracy with which the models could reproduce the true end-point population trends based on the true trajectory and compared the absolute difference between the estimated trend and the true trend for the spatial and non-spatial versions of the models. We estimated long-term trends using all six possible 50-year trend periods (i.e., 1966-2016, 1967-2017…, 1971-2021) in the simulated trajectories, and short-term trends using all possible 10-year trends. For both trajectories and trends, we also assessed estimation accuracy separately for strata near the core and periphery of the simulated species range. We separated peripheral and core strata because patterns of abundance and population change were most distinct and generally had lower abundance in the peripheral strata. We defined peripheral strata as the strata in the northern and southern parts of the range, specifically those with latitude centroids more than 1 SD away from the mean latitude of all strata centroids. In addition to comparing the spatial and non-spatial versions of the first-difference model, we also fitted and compared estimates from a non-hierarchical version of this model, where trends and abundance were estimated independently among strata, to demonstrate the benefits of sharing information on the status and trend parameters (see Supplementary).

Real Data Applications

We fit the models to real data from three broad-scale long-term monitoring programs. We used real data for the Eastern Whip-poor-will (*Antrostomus vociferus*) from the BBS, American Dipper (*Cinclus mexicanus*) from the CBC, and Red Knot (*Calidris canutus*) from the MSS monitoring data. Each of these programs required some elaborations to the model structure to account for particular aspects of each survey, such as effects that account for variation among observers, variation in effort, or variations due to the seasonal pattern in migration movements. For all models, the underlying abundance and population trajectory components were as described above, the specific elaborations that apply to each survey have been described in other work (Soykan et al. 2016, Meehan et al. 2019, Link et al. 2020, Smith and Edwards 2020), and we describe the detailed, survey-specific components of the models in the supplemental material.

We also used data from the BBS for Wood Thrush (*Hylocichla mustelina*) to apply the spatial models using a much finer spatial resolution than usually used for the BBS. The BBS design relies on a 1x1 degree latitude by longitude grid, within which routes are established using a stratified random design. We can stratify the data and estimate trends and abundances within each of these latitude by longitude grid cells with reasonable precision and accuracy by incorporating the spatial information. To demonstrate this fine-scale application of the models, we used data from the BBS for Wood Thrush from 2000 through 2021. We fit the first difference and GAMYE models, as well as a simpler GAM non-linear smooth without the annual fluctuations, to these Wood Thrush data and show the estimated trajectories and trend maps.

Fitting Details

The models here were all fit using the Stan probabilistic programming language (Stan Development Team 2022), accessed through the R-package cmdStanR (Gabry and Češnovar 2021). We drew between 1000-2000 samples from the posterior for each of the 4 independent chains after an approximately equal number of warm-up samples. There were no divergent transitions in any of the model applications, and we set the number of warm-ups and iterations to ensure that split-Rhat values were < 1.02 for all parameters in the models, and bulk effective sample sizes were always > 400 (Gelman et al. 2020, Vehtari et al. 2021). For all temporal parameters, including spline parameters ($\beta_{i,k}$, $\beta'_{i,k}$, and B_k), differences ($\pi_{i,t}$), and their associated variance terms, we used stricter thresholds so that effective sample sizes were > 1000. Similarly, for all estimated annual indices of abundance (the $n_{i,t}$, $nSmooth_{i,t}$, and $NSmooth_t$ parameters, from which all trend and trajectory inference are drawn), bulk effective sample sizes were all > 1000. These fully Bayesian hierarchical models require significant computational time to fit; the models we used required anywhere from 4 - 15 hours to run, depending on the species, dataset, and model (running on a Windows 11 computer, with chains run in parallel and using the Windows Subsystem for Linux option within cmdstan).

RESULTS

All the models, both non-spatial and spatial versions, reliably estimated the true population trajectories of the simulated data (Figure 2). The spatial models' trajectories were closer to the true trajectories than the non-spatial models (Figure 2). The spatial models' trends were more accurate than the non-spatial models (Figure 3) when and where the data were relatively sparse, such as in strata more on the periphery of the species' distribution (Figures 2 and 3). The estimated trajectories and trends were generally very similar amongst the models for strata at the core of the range and when there were more data, including strata with more routes, years with more observations, or simulated data sets with higher mean counts (Figures 2 and 3).

When applied to real data, the spatial model estimates show some interesting spatial patterns in population change for the three example species (Figures 4 and 5, with standard error plotted in figures S4 and S5); patterns that are not nearly as apparent in the non-spatial versions of the models. For the Eastern Whip-poor-will data (Figure 4), the spatial GAMYE models show that the relatively slow decline between approximately 1970 and 1980 was a mixture of declining populations in the Appalachian and north-central parts of the species' range and increases elsewhere; during 1995-2005, the steep declines were seen everywhere, and the more recent relatively stable population appears to be a balance of increases in the Appalachian and northern parts of the range and decreases elsewhere. These spatial patterns in population change are not as evident in the non-spatial models and yet the overall population trajectories from the two models are very similar (Figure 4). The spatial patterns and the contrast between the spatial and non-spatial models are almost identical for the first-difference models applied to the Eastern Whip-poor-will data (Figure S4).

The survey-wide declines in Red Knot populations from MSS (Figure 5) are reflected in both GAMYE models, but the north-south separation in trend during the 1980s is only apparent in the spatial version. For the American Dipper data in the CBC, the estimates from the spatial and non-spatial first-difference models are generally quite similar, but the spatial models suggest that in the 1970s, the species was generally decreasing in the northern part of its range and increasing in the South (not shown) and that pattern reversed in the early 2000s (Figure 5).

The spatial distribution of trends for Wood Thrush at a fine spatial resolution (strata defined by grid-cells of 1-degree latitude and longitude) suggest that between 2007 and 2021 (matching the time-period available for comparison to eBird status and trends (Fink et al. 2022), species' populations have increased in the eastern portions of its range, approximately following the Mississippi Valley, are relatively stable throughout the Appalachian regions, and are generally decreasing elsewhere (Figure 6 with standard errors plotted in Figure S6). We have plotted the trend map based on results from the first difference model, but they are almost identical to the patterns and standard errors estimated using the GAMYE or a simpler GAM model (Figure S7).

DISCUSSION

Sharing spatially explicit information across a species' range improves estimates of wildlife population status and trend by sharing information on the most important model parameters: those that represent abundance and temporal changes in abundance (trend). Explicitly spatial models improve our estimates of status and trends by better tracking the spatially dependent processes that affect wildlife populations (Ver Hoef et al. 2018). By sharing information across space and time, regions and periods with relatively sparse data (e.g., northern Canada, the periphery of species' ranges, and/or the early years of the survey) are better estimated (Carroll et al. 2010, Bled et al. 2013). Similarly, estimates for species with sparse data are more robust because the spatial information reduces the effects of sampling noise in each stratum, improving the hyperparameter and/or composite trend, effectively increasing the amount of information per strata (Figure 3; Bled et al. 2013). The improvement of population estimates made with fewer data is especially important for assessments of species conservation status, as the time periods used to evaluate declines are short. For example, the Committee on the Status of Endangered Wildlife in Canada (COSEWIC), determines status based on declines occurring within 10 years or 3 generations (Government of Canada 2014). Spatial models also tell an intuitive story, with maps that smooth trend variation spatially, highlighting regions with similar trends (Figure 4, Figure 5; Ver Hoef et al. 2018). Smooth maps of trends make it easier to develop hypotheses, understand community drivers, convey regional patterns, or identify areas of conservation interest.

Spatially explicit models better capture spatial drivers of population change. The resulting maps more clearly reflect spatial patterns, facilitating the pairing of trend to spatial drivers and facilitating hypothesis generation for subsequent research. For example, the spatial model's predictions for the Eastern Whip-poor-will shows patterns that align with geophysical features such as the Appalachian Mountains (Figure 4). Thereby, suggesting that further study of processes related to elevation may help understand population drivers. The CBC American Dipper trend models (Figure 5) show consistent increases in the north (above the 40th parallel) in the spatial models; a latitudinal pattern that may suggest further study of climate-driven processes (Murrish 1970, Nilsson et al. 2011, Sullivan and Vierling 2012, Saunders et al. 2022). The Wood Thrush spatial model had consistent increases through the western edge of their range (Figure 6), perhaps suggesting that drivers associated with the Mississippi River basin are worth investigating (Yasarer et al. 2020), or stimulating additional work on delimiting natural populations or exploring drivers across the annual cycle (Rushing et al. 2016).

The underlying assumption of spatial models is intuitive, allowing for clear visualizations. Spatial models reflect both the non-independence of population processes within a species' range and the inherently spatial nature of ecological processes (Ver Hoef et al. 2018). Sharing information across a region reduces the emphasis on individual estimates, which is especially important when those estimates are imprecise (Link and Sauer 2002). The partial pooling of information among strata reflects the skepticism of knowledgeable users of population trends (i.e., biologists and population mangers) when interpreting local trends that are extreme relative to range-wide trends. The Eastern Whip-poor-will trend maps demonstrate this, with the non-spatial model having a patchwork of increases and decreases, particularly in the North (Figure 4). By contrast, the spatial model for the Eastern Whip-poor-will produces a map with only increases in the north (Figure 4). For the trend maps produced using CBC and MSS data, the spatial models showed more consistent patterns, with regions of solid increase and decrease that are not present in the non-spatial versions (Figure 5).

Spatial, hierarchical models using smaller strata (Figure 6, Figure S7) allow for finer-grain spatial inference on the patterns of population change and allow for a wide range of covariates. The small strata used here and in previous studies (Meehan et al. 2019) reduce influence of the somewhat arbitrary structure imposed by using political divisions (i.e. states, provinces) or larger stratifications that may not be as relevant to individual species, such as the Bird Conservation Regions (Link et al. 2006, 2020; Smith and Edwards 2020). Hierarchical structuring also creates finer timescale trends (Figure 2), which combined with the small strata, allow for the inclusion of finer-scale covariates in time and space (Carroll et al. 2010). More localized covariates could include the amount of habitat or the pesticide use in the neighborhood, both of which affect species distributions (Thogmartin et al. 2004, Stanton et al. 2018, Betts et al. 2022). Smaller time-scale covariates could be the wetness of the previous spring or the previous year's prey abundance (Wilson et al. 2018, Stanton et al. 2018).

Our models share information across both time and space, which improves estimates, particularly in data-sparse situations. The spatial models especially outperform the non-spatial models when there are fewer bird counts and in the peripheral strata (Figure 3). Data-sparse situations can be due to isolated strata, such as northern North America, which has few BBS routes compared to the southern regions (Downes et al. 2016). Data-sparse situations may also be due to short time periods, such as tracking population declines over a 10-year period, which is used in Canada to designate conservation risk (Government of Canada 2014) and used internationally to assign IUCN red list status (IUCN 2012). Further, population estimates for a small area is another data-sparse situation. In all these cases, sharing information across space and time increases the amount of information available to inform conclusions about population change.

Our hierarchical models assume that trends within strata are not independent of trends across the species range (Cressie et al. 2009), which may not always be appropriate. If a study is interested in estimating differences in trends among strata, or there is a biological reason to suggest that trends in some parts of the species' range are independent of those in the rest of the range, then the assumptions of the hierarchical or spatial model may not be met. Hierarchical models have group and global smoothers and concurve smoothers may even cancel each other out and create a flat trendline (Morrison et al. 2010, Pedersen et al. 2019). Further, if the area of interest is data-poor compared to the rest of the region, trends may be pulled closer to the rest of the region. In terms of the spatial models, a stratum with missing data could be artificially connected to its closest neighbors, forcing a spatial connection when it is, in fact, an island (Freni-Sterrantino et al. 2018). In this case, using multiple separate spatial networks may be the best solution (Freni-Sterrantino et al. 2018). Ultimately, the design of the model and the hierarchical and spatial priors must align with the study question, and no model is ideally suited to all questions.

One complication of the spatial, iCAR models is that they often require some decisions about how to treat disconnected neighbor graphs (Freni-Sterrantino et al. 2018). For example, the MSS data are collected at sites that are not continuously distributed in space and so for any stratification based on a regular grid, there will be multiple strata with missing data. Similarly, for the CBC and BBS data, there are many species where a particular stratification of their data results in a disconnected neighborhood graph. Here, we used a Voronoi tessellation to force a fully connected network if needed (e.g., MSS data for Red Knot). This approach may not be ideal, as it distorts the Euclidean distances and neighborhood relationships among strata. It is a pragmatic solution that improves on a simple hierarchical structure that is completely naïve to spatial location by allowing the model to understand relative spatial location, so that otherwise disconnected strata can share information from the nearest strata. Ultimately, any areal stratification necessitates a distortion of Euclidean space because, for the monitoring programs here, the observations are collected at a subset of smaller areas or linear transects within each stratum. Alternatively, we could consider adding the missing strata to the model, keeping the true neighborhood relationships, and estimating the additional parameters for those missing strata (Meehan et al. 2019).

Estimates from the spatial models here could be compared to the spatially structured trend estimates created with eBird data (Figure 6, Figure S7; Pacifici et al. 2017, Fink et al. 2022). Our parametric models, using structured monitoring data during the breeding season, non-breeding season, and migration, provide spatial information on population trends that can be compared to the spatial patterns in trends from the machine learning models using the less-structured data of eBird. eBIRD is a citizen science initiative with an enormous collection of birdwatchers' observations (Sullivan et al. 2014), but is not sampled in a standardized way like the other datasets described here. Comparisons of the spatial patterns using the different data sources and modeling approaches should help inform our understanding of the spatially dependent factors influencing population change as well as understand the data or analytical factors that may lead to differences. In general, the spatial patterns in Wood Thrush (*Hylocichla mustelina*) trends from the BBS and eBird (Fink et al. 2022) show some clear similarities. Comparably scaled estimates of trends from the BBS data for any other species can be made using the R package bbsBayes2 (Edwards et al. 2023) using the GAMYE and first-difference models for comparison to estimates from eBird.

Future work could investigate and summarize the spatial patterns in trends for specific guilds of birds, such as insectivores, with group-specific smoothers, extending the hierarchical priors to multi-species models. Multi-species summaries from species-specific models (North American Bird Conservation Initiative Canada 2019, Rosenberg et al. 2019) could be informative, as could multi-species versions of the spatial models here. It would be reasonable to assume that spatial patterns in trends should be similar for species responding to shared, spatially dependent processes, such as changes in landcover, human activity, and climate. Covariates such as land cover, land use, and climate could be included to estimate their effects on trends while adjusting for other spatially dependent processes. Models that explicitly estimate a spatial surface of trends may also provide an easier way to integrate monitoring information among datasets with variations in their level of structure, observation, and counting processes, such as species-specific monitoring programs, waterfowl breeding population surveys, BBS, and eBIRD observations (Joseph et al. 2021).

Hierarchical, spatial models are valuable tools for conservation planning and wildlife management. These models share information within species and amongst neighboring regions, creating fine-scale models (Figure 6). Many biotic and abiotic factors act at small scales (Thogmartin et al. 2004, Paton et al. 2019, Monroe et al. 2022), requiring fine-scale modeling. For conservation purposes, fine scale models can be used to evaluate protected areas' effects (Donnelly et al. 2017), predict invasive species distributions (Latimer et al. 2009), track population trends, and determine drivers of population change (Meehan et al. 2019). The models implemented in this study can be applied to a wide range of questions and be used to guide conservation decisions.

LITERATURE CITED

Albers, S. (2022). rsoi: Import Various Northern and Southern Hemisphere Climate Indices.

Audubon (2022). Christmas Bird Count. [Online.] Available at https://netapp.audubon.org/cbcobservation/.

Besag, J., J. York, and A. Mollié (1991). Bayesian image restoration, with two applications in spatial statistics. Annals of the Institute of Statistical Mathematics 43:1–20.

Betts, M. G., Z. Yang, A. S. Hadley, A. C. Smith, J. S. Rousseau, J. M. Northrup, J. J. Nocera, N. Gorelick, and B. D. Gerber (2022). Forest degradation drives widespread avian habitat and population declines. Nature Ecology & Evolution 6:709–719.

Birds Canada (2023). NatureCounts. [Online.] Available at https://naturecounts.ca/nc/default/searchquery.jsp.

Bled, F., J. Sauer, K. Pardieck, P. Doherty, and J. A. Royle (2013). Modeling Trends from North American Breeding Bird Survey Data: A Spatially Explicit Approach. PLoS ONE 8.

Bürkner, P.-C. (2017). brms: An R Package for Bayesian Multilevel Models Using Stan. Journal of Statistical Software 80:1–28.

Carroll, C., D. S. Johnson, J. R. Dunk, and W. J. Zielinski (2010). Hierarchical Bayesian Spatial Models for Multispecies Conservation Planning and Monitoring. Conservation Biology 24:1538–1548.

Cressie, N., C. A. Calder, J. S. Clark, J. M. V. Hoef, and C. K. Wikle (2009). Accounting for uncertainty in ecological analysis: the strengths and limitations of hierarchical statistical modeling. Ecological Applications 19:553–570.

Donnelly, J. P., J. D. Tack, K. E. Doherty, D. E. Naugle, B. W. Allred, and V. J. Dreitz (2017). Extending Conifer Removal and Landscape Protection Strategies from Sage-grouse to Songbirds, a Range-Wide Assessment. Rangeland Ecology & Management 70:95–105.

Downes, C. M., M.-A. Hudson, A. C. Smith, and C. M. Francis (2016). The Breeding Bird Survey at 50: scientists and birders working together for bird conservation. Avian Conservation and Ecology 11.

eBIRD (2022). Download eBird data products - eBird Science. [Online.] Available at https://science.ebird.org/en/use-ebird-data/download-ebird-data-products.

Edwards, B. P. M., and A. C. Smith (2021). bbsBayes: An R Package for Hierarchical Bayesian Analysis of North American Breeding Bird Survey Data. Journal of Open Research Software 9:19.

Edwards, B. P. M., A. C. Smith, and S. LaZerte (2023). bbsBayes2. [Online.] Available at https://github.com/bbsBayes/bbsBayes2.

Fewster, R. M., S. T. Buckland, G. M. Siriwardena, S. R. Baillie, and J. D. Wilson (2000). Analysis of Population Trends for Farmland Birds Using Generalized Additive Models. Ecology 81:1970–1984.

Finch, T., S. J. Butler, A. M. A. Franco, and W. Cresswell (2017). Low migratory connectivity is common in long-distance migrant birds. Journal of Animal Ecology 86:662–673.

Fink, D., A. Johnston, M. Strimas-Mackey, T. Auer, W. M. Hochachka, S. Ligocki, L. O. Jaromczyk, O. Robinson, C. Wood, S. Kelling, and A. D. Rodewald (2022). A Double Machine Learning Trend Model for Citizen Science Data. [Online.] Available at http://arxiv.org/abs/2210.15524.

Freni-Sterrantino, A., M. Ventrucci, and H. Rue (2018). A note on intrinsic conditional autoregressive models for disconnected graphs. Spatial and Spatio-temporal Epidemiology 26:25–34.

Gabry, J., and R. Češnovar (2021). R Interface to CmdStan. [Online.] Available at https://mc-stan.org/cmdstanr/.

Gabry, J., and B. Goodrich (no date). Bayesian Applied Regression Modeling via Stan. [Online.] Available at https://mc-stan.org/rstanarm/.

Gelman, A., A. Vehtari, D. Simpson, C. C. Margossian, B. Carpenter, Y. Yao, L. Kennedy, J. Gabry, P.-C. Bürkner, and M. Modrák (2020). Bayesian Workflow. arXiv:2011.01808 [stat].

Government of Canada (2014). COSEWIC quantitative criteria and guidelines for the Status Assessment of Species: table 2. [Online.] Available at https://www.canada.ca/en/environment-climate-change/services/species-risk-act-accord-funding/listing-process/quantitative-criteria-guidelines-status-table-2.html.

Hill, J. M., J. F. Egan, G. E. Stauffer, and D. R. Diefenbach (2014). Habitat Availability Is a More Plausible Explanation than Insecticide Acute Toxicity for U.S. Grassland Bird Species Declines. PLOS ONE 9:e98064.

Howe, M. A., P. H. Geissler, and B. A. Harrington (1989). Population trends of North American shorebirds based on the International Shorebird Survey. Biological Conservation 49:185–199.

IUCN (2001). International Union for Conservation of Nature, Natural Resources. Species Survival Commission, & IUCN Species Survival Commission. IUCN Red List categories and criteria.

IUCN (2012). IUCN Red List Categories and Criteria: Version 3.1. 2nd edition. IUCN, Gland, Switzerland and Cambridge, UK.

Joseph, M. B., D. C. P. Jr, and A. M. Bartuszevige (2021). Data fusion for abundance estimation: community science augments systematically collected removal-in-time distance sampling data. 26.

van Klink, R., D. E. Bowler, K. B. Gongalsky, A. B. Swengel, A. Gentile, and J. M. Chase (2020). Meta-analysis reveals declines in terrestrial but increases in freshwater insect abundances. Science 368:417–420.

Koenig, W. D., and A. M. Liebhold (2016). Temporally increasing spatial synchrony of North American temperature and bird populations. Nature Climate Change 6:614–617.

Latimer, A. M., S. Banerjee, H. Sang Jr, E. S. Mosher, and J. A. Silander Jr (2009). Hierarchical models facilitate spatial analysis of large data sets: a case study on invasive plant species in the northeastern United States. Ecology Letters 12:144–154.

Link, W. A., and J. R. Sauer (2002). A Hierarchical Analysis of Population Change with Application to Cerulean Warblers. Ecology 83:2832–2840.

Link, W. A., J. R. Sauer, and D. K. Niven (2006). A Hierarchical Model for Regional Analysis of Population Change Using Christmas Bird Count Data, with Application to the American Black Duck. The Condor 108:13–24.

Link, W. A., J. R. Sauer, and D. K. Niven (2017). Model selection for the North American Breeding Bird Survey: A comparison of methods. The Condor 119:546–556.

Link, W. A., J. R. Sauer, and D. K. Niven (2020). Model selection for the North American Breeding Bird Survey. Ecological Applications 30:e02137.

Meehan, T. D., N. L. Michel, and H. Rue (2019). Spatial modeling of Audubon Christmas Bird Counts reveals fine-scale patterns and drivers of relative abundance trends. Ecosphere 10:e02707.

Michel, N. L., K. A. Hobson, C. A. Morrissey, and R. G. Clark (2021). Climate variability has idiosyncratic impacts on North American aerial insectivorous bird population trajectories. Biological Conservation 263:109329.

Michel, N. L., A. C. Smith, R. G. Clark, C. A. Morrissey, and K. A. Hobson (2016). Differences in spatial synchrony and interspecific concordance inform guild-level population trends for aerial insectivorous birds. Ecography 39:774–786.

Miller, D. L., D. Fifield, E. Wakefield, and D. B. Sigourney (2021). Extending density surface models to include multiple and double-observer survey data. PeerJ 9:e12113.

Monroe, A. P., J. A. Heinrichs, A. L. Whipple, M. S. O'Donnell, D. R. Edmunds, and C. L. Aldridge (2022). Spatial scale selection for informing species conservation in a changing landscape. Ecosphere 13:e4320.

Morris, M., K. Wheeler-Martin, D. Simpson, S. J. Mooney, A. Gelman, and C. DiMaggio (2019). Bayesian hierarchical spatial models: Implementing the Besag York Mollié model in stan. Spatial and Spatio-temporal Epidemiology 31:100301.

Morrison, C. A., R. A. Robinson, J. A. Clark, and J. A. Gill (2010). Spatial and temporal variation in population trends in a long-distance migratory bird. Diversity and Distributions 16:620–627.

Morrison, C. A., R. A. Robinson, J. A. Clark, K. Risely, and J. A. Gill (2013). Recent population declines in Afro-Palaearctic migratory birds: the influence of breeding and non-breeding seasons. Diversity and Distributions 19:1051–1058.

Morrison, R. I. G., C. Downes, and B. Collins (1994). Population Trends of Shorebirds on Fall Migration in Eastern Canada 1974-1991. The Wilson Bulletin 106:431–447.

Murrish, D. E. (1970). Responses to temperature in the dipper, Cinclus mexicanus. Comparative Biochemistry and Physiology 34:859–869.

Nilsson, A. L. K., E. Knudsen, K. Jerstad, O. W. Røstad, B. Walseng, T. Slagsvold, and N. C. Stenseth (2011). Climate effects on population fluctuations of the white-throated dipper Cinclus cinclus. Journal of Animal Ecology 80:235–243.

North American Bird Conservation Initiative Canada (2019). The State of Canada's Birds, 2019. Environment and Climate Change Canada.

North American Bird Conservation Initiative U.S. Committee (2000). North American Bird Conservation Initiative: Bird Conservation Region descriptions, a supplement to the North American Bird Conservation Initiative Bird Conservation Regions map.

Pacifici, K., B. J. Reich, D. A. W. Miller, B. Gardner, G. Stauffer, S. Singh, A. McKerrow, and J. A. Collazo (2017). Integrating multiple data sources in species distribution modeling: a framework for data fusion*. Ecology 98:840–850.

Paton, G. D., A. V. Shoffner, A. M. Wilson, and S. A. Gagné (2019). The traits that predict the magnitude and spatial scale of forest bird responses to urbanization intensity. PLOS ONE 14:e0220120.

Pedersen, E. J., D. L. Miller, G. L. Simpson, and N. Ross (2019). Hierarchical generalized additive models in ecology: an introduction with mgcv. PeerJ 7:e6876.

Renfrew, R. B., D. Kim, N. Perlut, J. Smith, J. Fox, and P. P. Marra (2013). Phenological matching across hemispheres in a long-distance migratory bird. Diversity and Distributions 19:1008–1019.

Roberts, C. P., R. Scholtz, D. T. Fogarty, D. Twidwell, and T. L. Walker Jr. (2022). Large-scale fire management restores grassland bird richness for a private lands ecoregion. Ecological Solutions and Evidence 3:e12119.

Rosenberg, K. V., A. M. Dokter, P. J. Blancher, J. R. Sauer, A. C. Smith, P. A. Smith, J. C. Stanton, A. Panjabi, L. Helft, M. Parr, and P. P. Marra (2019). Decline of the North American avifauna. Science 366:120–124.

Ross, R. K., P. A. Smith, B. Campbell, C. A. Friis, and R. I. G. Morrison (2012). Population Trends of Shorebirds in Southern Ontario, 1974–2009. Waterbirds 35:15–24.

Rushing, C. S., T. B. Ryder, and P. P. Marra (2016). Quantifying drivers of population dynamics for a migratory bird throughout the annual cycle. Proceedings of the Royal Society B: Biological Sciences 283:20152846.

Sauer, J. R., and W. A. Link (2011). Analysis of the North American Breeding Bird Survey Using Hierarchical ModelsAnálisis de los Censos de Aves Reproductivas de Norte América Mediante Modelos Jerárquicos. The Auk 128:87–98.

Saunders, S. P., T. D. Meehan, N. L. Michel, B. L. Bateman, W. DeLuca, J. L. Deppe, J. Grand, G. S. LeBaron, L. Taylor, H. Westerkam, J. X. Wu, and C. B. Wilsey (2022). Unraveling a century of global change impacts on winter bird distributions in the eastern United States. Global Change Biology n/a.

Smith, A. C. (2023). Spatial_Hierarchical_Trend_Models. [Online.] Available at https://github.com/AdamCSmithCWS/Spatial_Hierarchical_Trend_Models.

Smith, A. C., and B. P. M. Edwards (2020). North American Breeding Bird Survey status and trend estimates to inform a wide range of conservation needs, using a flexible Bayesian hierarchical generalized additive model. The Condor. https://doi.org/10.1093/ornithapp/duaa065

Smith, A. C., M.-A. R. Hudson, C. Downes, and C. M. Francis (2014). Estimating breeding bird survey trends and annual indices for Canada: how do the new hierarchical Bayesian estimates differ from previous estimates? The Canadian Field-Naturalist 128:119–134.

Smith, P. A., A. C. Smith, B. Andres, C. M. Francis, B. Harrington, C. Friis, R. I. G. Morrison, J. Paquet, B. Winn, and S. Brown (2023). Accelerating declines of North America’s shorebirds signal the need for urgent conservation action. Ornithological Applications:duad003.

Soykan, C. U., J. Sauer, J. G. Schuetz, G. S. LeBaron, K. Dale, and G. M. Langham (2016). Population trends for North American winter birds based on hierarchical models. Ecosphere 7:e01351.

Sponsler, D. B., F. Requier, K. Kallnik, A. Classen, F. Maihoff, J. Sieger, and I. Steffan-Dewenter (2022). Contrasting patterns of richness, abundance, and turnover in mountain bumble bees and their floral hosts. Ecology 103:e3712.

Stan Development Team (2022). Stan. *stan-dev.github.io*. [Online.] Available at //mc-stan.org/about/team/.

Stanton, R. L., C. A. Morrissey, and R. G. Clark (2018). Analysis of trends and agricultural drivers of farmland bird declines in North America: A review. Agriculture, Ecosystems & Environment 254:244–254.

Sullivan, B. L., J. L. Aycrigg, J. H. Barry, R. E. Bonney, N. Bruns, C. B. Cooper, T. Damoulas, A. A. Dhondt, T. Dietterich, A. Farnsworth, D. Fink, et al. (2014). The eBird enterprise: An integrated approach to development and application of citizen science. Elsevier 169:31–40.

Sullivan, S. M. P., and K. T. Vierling (2012). Exploring the influences of multiscale environmental factors on the American dipper Cinclus mexicanus. Ecography 35:624–636.

Thogmartin, W. E., J. R. Sauer, and M. G. Knutson (2004). A Hierarchical Spatial Model of Avian Abundance with Application to Cerulean Warblers. Ecological Applications 14:1766–1779.

U.S. Geological Survey, and Canadian Wildlife Services (2021). Raw Data - USGS Patuxent Wildlife Research Center. [Online.] Available at https://www.pwrc.usgs.gov/bbs/RawData/.

Vehtari, A., A. Gelman, D. Simpson, B. Carpenter, and P.-C. Bürkner (2021). Rank-Normalization, Folding, and Localization: An Improved Rˆ for Assessing Convergence of MCMC (with Discussion). Bayesian Analysis 16:667–718.

Ver Hoef, J. M., E. E. Peterson, M. B. Hooten, E. M. Hanks, and M.-J. Fortin (2018). Spatial autoregressive models for statistical inference from ecological data. Ecological Monographs 88:36–59.

Wilson, S., A. C. Smith, and I. Naujokaitis-Lewis (2018). Opposing responses to drought shape spatial population dynamics of declining grassland birds. Diversity and Distributions 24:1687–1698.

Wood, S. N. (2017). Generalized Additive Models: An Introduction with R. 2nd edition. Chapman and Hall/CRC.

Yasarer, L. M. W., J. M. Taylor, J. R. Rigby, and M. A. Locke (2020). Trends in Land Use, Irrigation, and Streamflow Alteration in the Mississippi River Alluvial Plain. Frontiers in Environmental Science 8.

Ziolkowski Jr., D., M. Lutmerding, V. Aponte, and M.-A. Hudson (2022). North American Breeding Bird Survey Dataset 1966-2021. [Online.] Available at https://www.sciencebase.gov/catalog/item/625f151ed34e85fa62b7f926.

Figure Captions

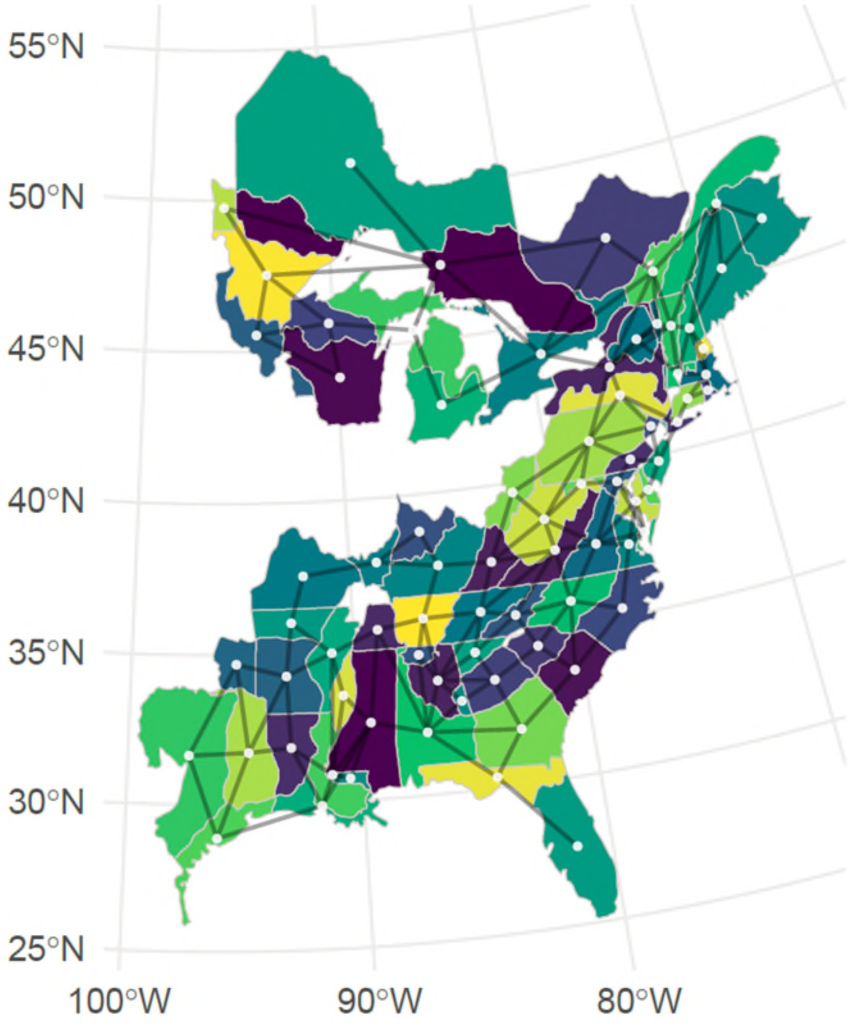

Figure 1. Spatial strata and lines indicating the neighboring relationships among the strata for all simulated data used in this study (based on Pine Warbler data from the BBS). The lines link the geographic centroids of each stratum's polygon(s) to the polygons that share an edge. Note: In some cases, the shared edges may not be immediately obvious because some strata include multiple polygons, and the centroids are included to aid in visualizing the links but may be slightly outside of polygons that have complex shapes.

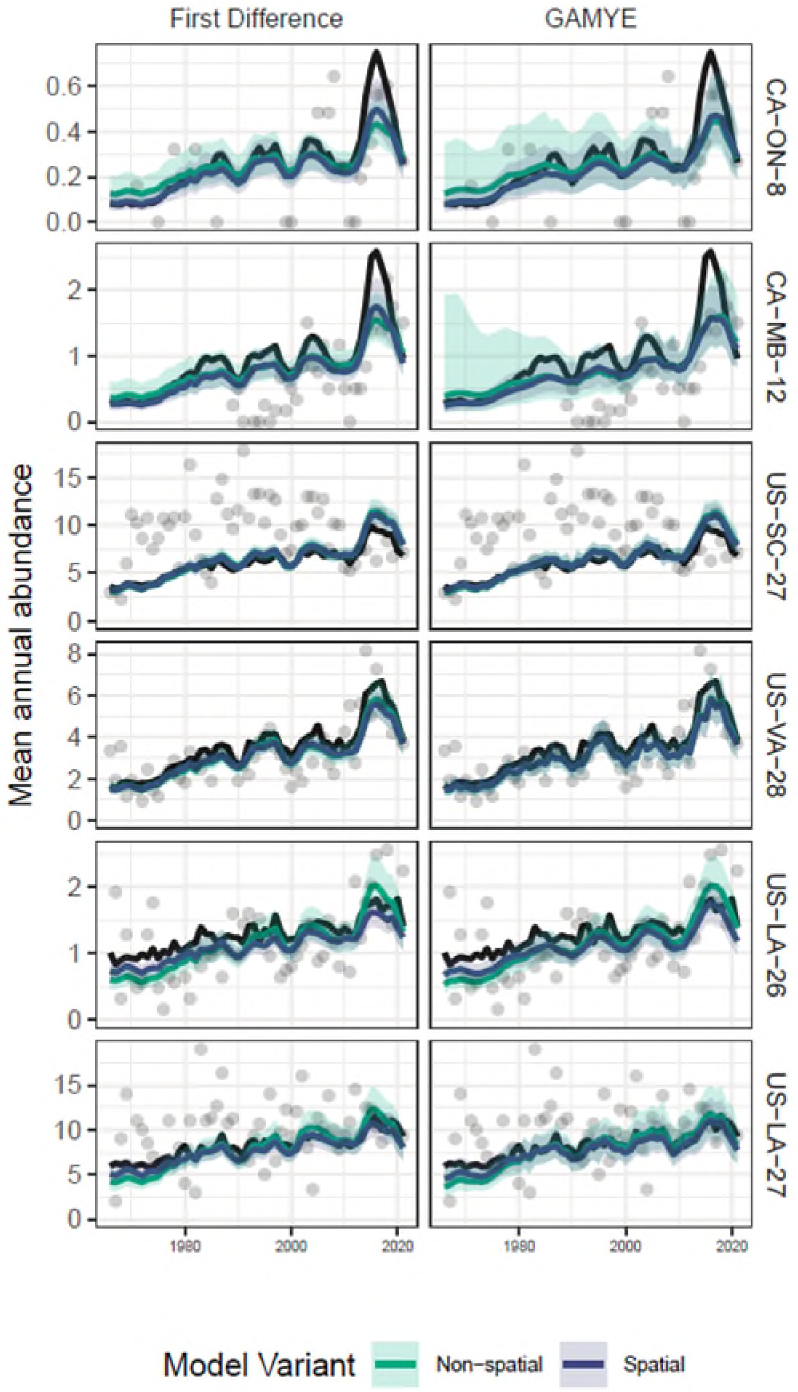

Figure 2. The estimated (colored lines and uncertainty bands) and true (black lines) population trajectories from spatial and non-spatial models for simulated bird monitoring data, based on counts from observers at sites within geographic strata. The six example strata shown here

represent two strata from the northern periphery of the simulated species' range (upper two plots), two from the core of the range (middle two), and two from the southern periphery (bottom two). Estimates for the core of the species' range are most similar among models and to the true trajectories. Estimates for strata on the periphery of the range show that estimates from the spatial models are more similar to the true trajectories than the non-spatial. The grey dots represent the annual means of the simulated data used to fit the models (i.e., mean counts each year from the observers and sites with data). The northern strata also provide examples of relatively data-sparse situations where there are few surveys (e.g., many years with zero observed birds in the top plot and no surveys at all before 1989 in the second plot).

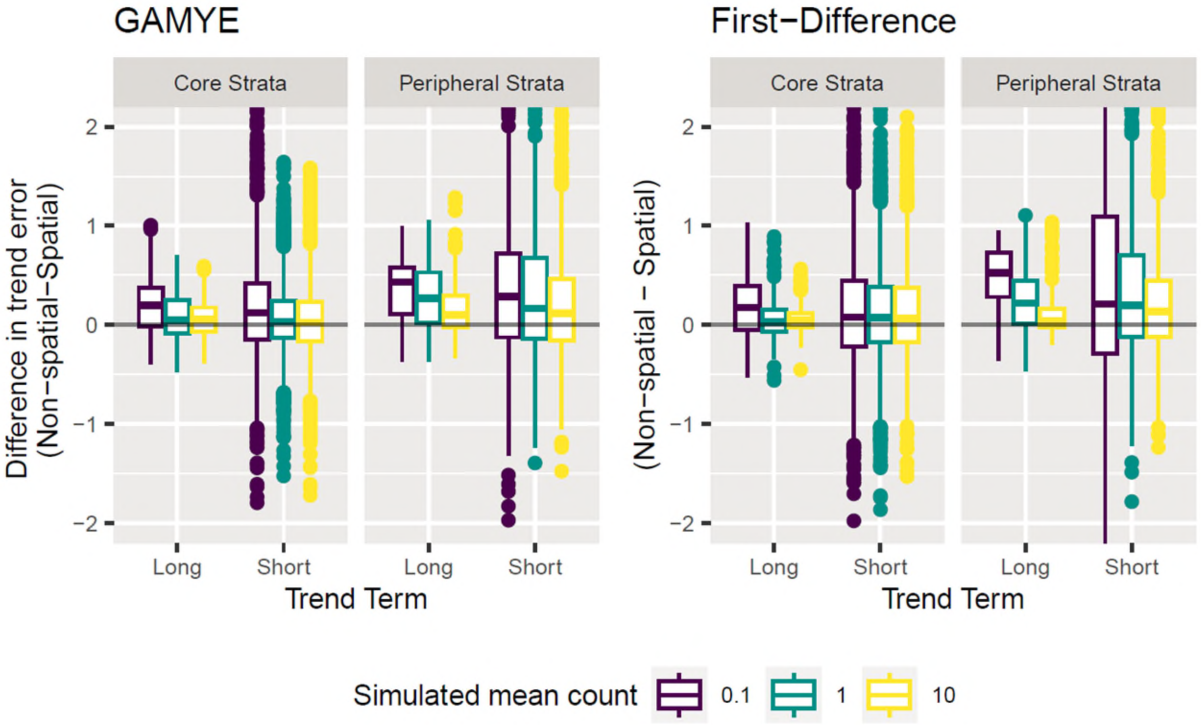

Figure 3. Difference in absolute error of trend estimates between spatial and non-spatial versions of the GAMYE and first difference models for the simulated data (left and center plots). The box and whisker plots represent the distribution of percent/year differences in absolute error (hierarchical - spatial) for trends in each stratum and each length of time (long-term and short-term), so that positive values indicate the spatial model estimates were more accurate (lower error). The colors represent different mean counts of the simulated data (0.1, 1, and 10 birds per survey).

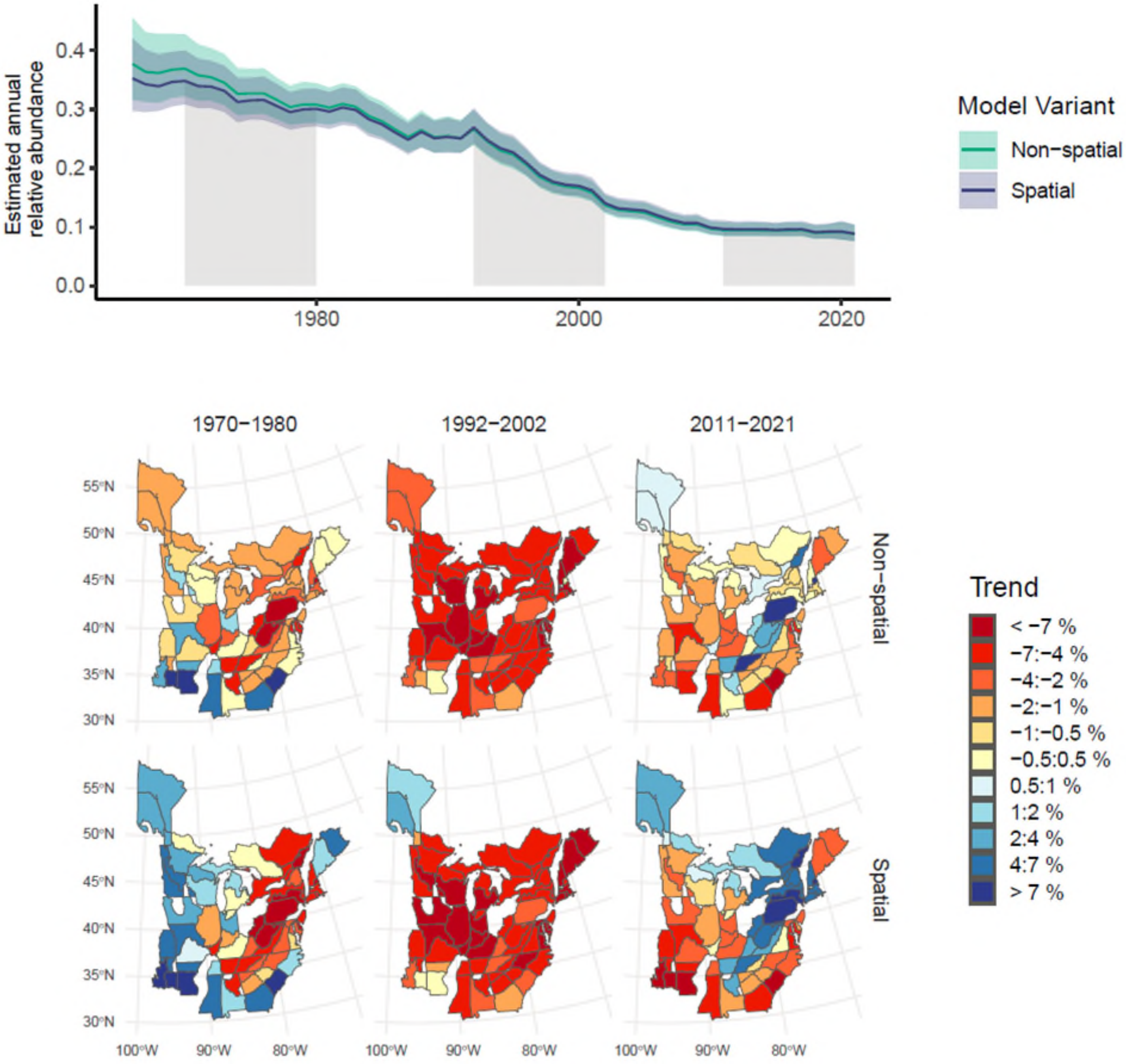

Figure 4. Estimated survey-wide population trajectories and spatial patterns in trends for Eastern Whip-poor-will from the North American Breeding Bird Survey (BBS) from non-spatial and spatial versions of the GAMYE model. The trend maps for selected 10-year trend periods highlight the spatial patterns in trends that are evident from the spatial version of the model and yet have a little effect on the overall population trajectory.

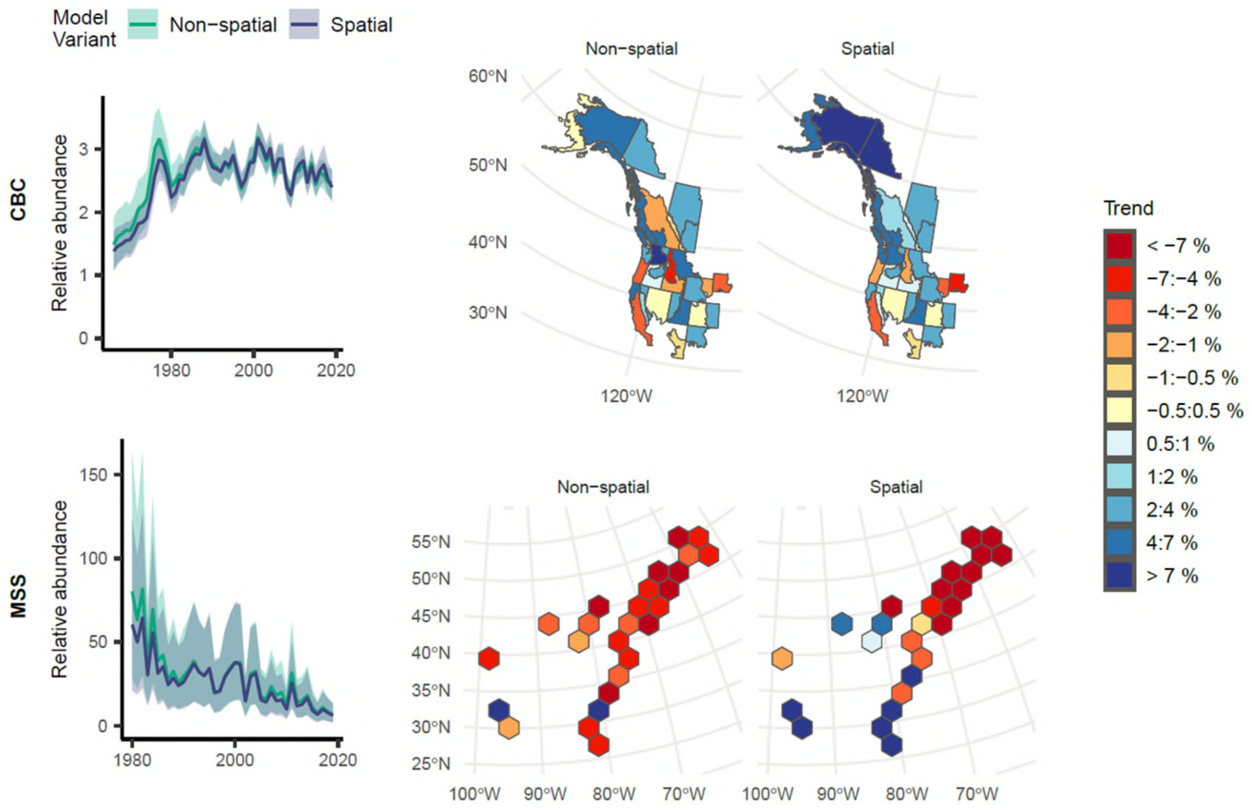

Figure 5. Estimated survey-wide population trajectories and maps of trend estimates for selection 10-year periods derived from non-spatial and spatial models applied to one dataset from the Christmas Bird Count (CBC, American Dipper), and one from the Migrating Shorebird Surveys (MSS, Red Knot). The overall population trajectories are relatively similar for the non-spatial and spatial models. The trend maps demonstrate the added spatial information on rates of population change that can be gleaned from the spatial versions of the models. Estimates for the CBC are derived from the first difference models, and those from the MSS are derived from the GAMYE models.

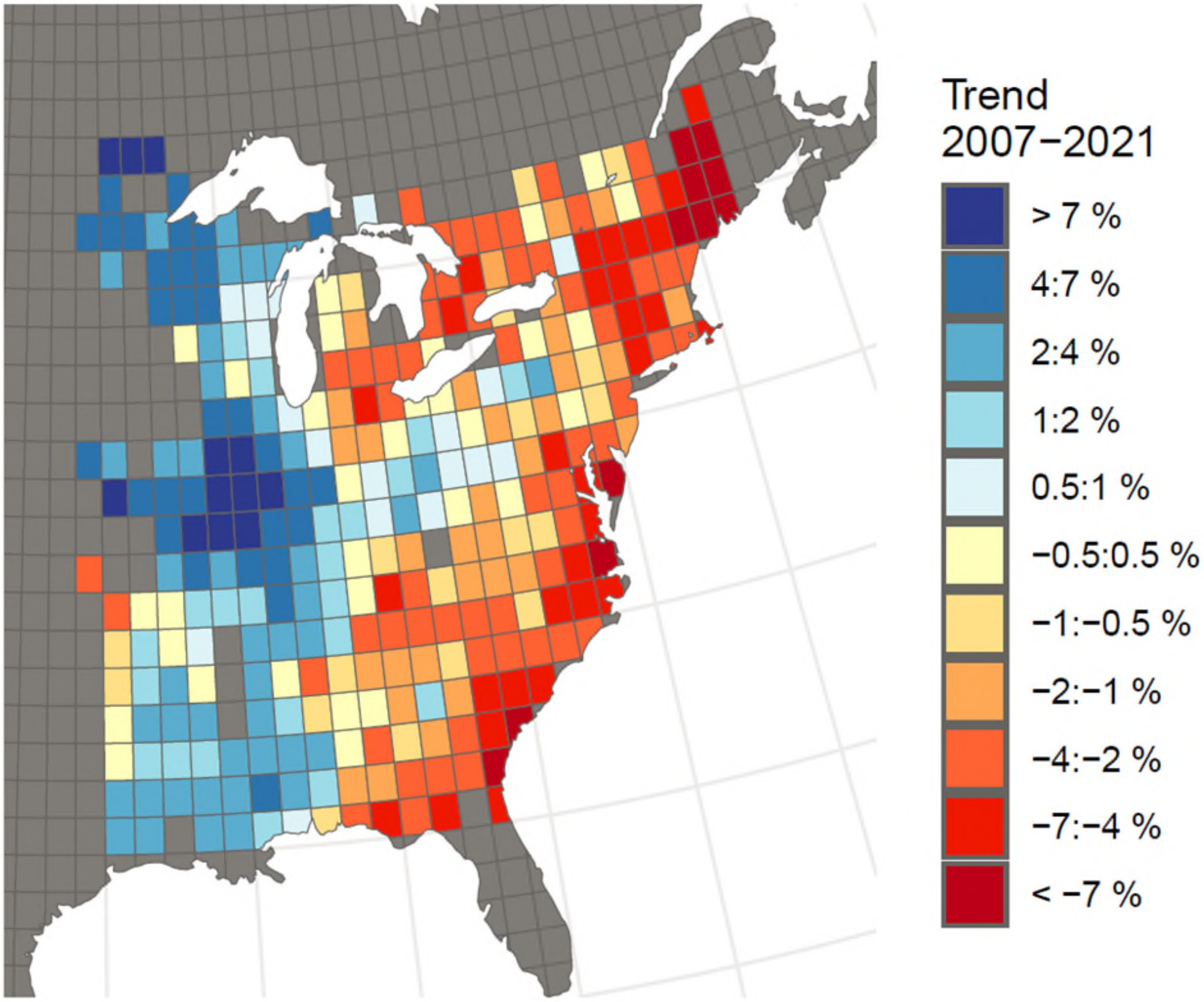

Figure 6. Estimated population trends for Wood Thrush from 2007-2021, from a spatial version of the first-difference model applied to Breeding Bird Survey (BBS) data stratified based on a 1 degree latitude by 1 degree longitude grid cells.

Supplement – Smith et al. spatial hierarchical population status and trend models

Contents:

- Supplemental methods
- Supplemental Results and Figures
- Priors and prior simulation results

Supplemental methods

BBS model

The BBS versions of the model included parameters to estimate the variation among observers (ω_o) and a parameter ($\eta I(o,j,t)$) to model the effect of an observer's first year of surveying a given route. This is similar to (Link and Sauer 2002) and other hierarchical models that have been applied to the BBS, except that here we have separate effects for observers and sites (routes in the BBS) and so the indicators ($I(o,j,t)$) are indexed by route-j, observer-o, and year-t.

$$log\left(\lambda_{j,i,t,o}\right) = \alpha_i + \Delta_{i,t} + \psi_j + \omega_o + \eta I(o,j,t) + \varepsilon_{j,i,t,o}$$

CBC model

The CBC version of the model included a non-linear effort correction, to account for the varying number of observers and time spent observing during an annual count (Soykan et al. 2016). The scaled effort value ($h_{i,j,t}$) represented the number of party hours as a proportion of the mean number of hours across all years and count circles. Parameters ν_i and ρ_i in the effort correction ($\frac{\nu_i\left(h_{i,j,t}^{\rho_i}-1\right)}{\rho_i}$) control the shape and direction of the relationship between effort and counts (Link et al. 2006), and they were estimated as varying effects among strata, centered on a mean hyperparameter ($\nu_i \sim N(N,\sigma_\nu^2)$, $\rho_i \sim N\left(P,\sigma_\rho^2\right)$).

$$log\left(\lambda_{j,i,t}\right) = \alpha_i + \Delta_{i,t} + \psi_j + \frac{\nu_i\left(h_{i,j,t}^{\rho_i}-1\right)}{\rho_i} + \varepsilon_{j,i,t}$$

MSS model

The migrating shorebird surveys version of the model was only fit as a GAMYE following Smith et al. (2023). It has a simplified parameterization for the year-effects (γ_t) so that year effects are the same across all strata ($\Delta_{i,t} = \delta_{i,t} + \gamma_t$), an extra smooth to account for variation in survey-timing during the migration season within two regions-r of the survey area ($\zeta_r(d)$), and an overall species intercept (α) only (i.e., no intercepts for the strata).

$$log\left(\lambda_{j,i,t,r,d}\right) = \alpha + \Delta_{i,t} + \psi_j + \zeta_r(d) + \varepsilon_{j,i,t,r,d}$$

This model differs from the CBC and BBS models largely because the survey monitors bird populations during the peak of their annual migrations, in comparison to relatively stationary populations monitored during either the breeding (BBS) or wintering (CBC) season. These migration-season data are extremely variable and require some simplifications to the estimation of year-effects, seasonal adjustments, and the survey-wide population trajectories and trends are estimated with the mean smooth (hyperparameter) because the relative counts of birds among regions and sites are not clearly representative of a given proportion of the population (Smith et al. 2023).

The year-effects in this model are common across all strata and sites, and so represent strong annual fluctuations with relatively consistent support across all strata in a given year. These could represent factors affecting a species' overall abundance in a given year, such as annual variations in breeding success, but would not capture more local or regional variations due to weather, annual variations in survey effort, or annual variation in the species' distribution during migration. We used a relatively informative prior on the standard deviation of the year-effects in the shorebird model ($\sigma_\gamma \sim |Normal(0,0.2)|$), so that 95% of the prior probability included annual fluctuations between a 33% decrease below the long-term trajectory and a 50% increase above the mean trajectory in any given year. Larger fluctuations are possible, when supported by the data, so we suggest this mildly informative prior is reasonable, given the survey-wide scale of the year-effects and the life history of most shorebird species.

The component of the shorebird model that adjusts for variation in mean counts over the course of the fall migration season ($\zeta_r(d)$) was estimated as a semi-parametric GAM smooth.

$$\zeta_r(d) = \sum_{\xi=1}^{\Xi} \theta_\xi \chi_{d,\xi}$$

We used the same type of basis function to estimate the seasonal smooth as we used for the smooth across years. We used $\Xi = 10$ knots, spread evenly over the 150-day season, to allow the seasonal pattern to be sufficiently flexible to accommodate more than a single peak, if supported by the data. We also fit a separate seasonal smooth for the strata in the Northern and Southern portions of the survey area for Red Knot, because migration timing tended to peak earlier in the Northern regions than in the Southern regions, but was relatively consistent across strata within each of the North and South.

Supplemental Results and Figures

Non-Hierarchical First-Difference Model

Our comparison of spatial and non-spatial models implicitly assumes that sharing information among strata on relative abundance and trends is meaningful. By contrast, some applications of hierarchical Bayesian status and trend models have been designed to avoid sharing information among strata on the trend and relative abundance parameters; to estimate trends independently among strata (Link et al. 2020). The first-difference model currently in use by the USGS to estimate status and trends from the BBS estimates the trends independently among strata; the temporal components are estimated in a non-hierarchical way. We also fit and compared estimates from this non-hierarchical version of the first-difference model to the spatial and non-spatial versions of the model for the BBS data and for the simulated data, as a demonstration of the costs and benefits of sharing information on the status and trend parameters.

For the simulated data, which included spatial structure in the abundance and trends, the non-hierarchical version of the first-difference model had higher absolute error (Figure S1). Using the same methods as we used to compare the spatial and non-spatial versions of the GAMYE and first-difference models, we compared the error in the trend estimates from the non-hierarchical first-difference to the error of the trend estimates from the non-spatial first-difference model. The non-hierarchical version of the first-difference model had higher error overall in the trend estimates than the non-spatial version, and the increase in error was similar in both the core and peripheral regions of the simulated species' range.

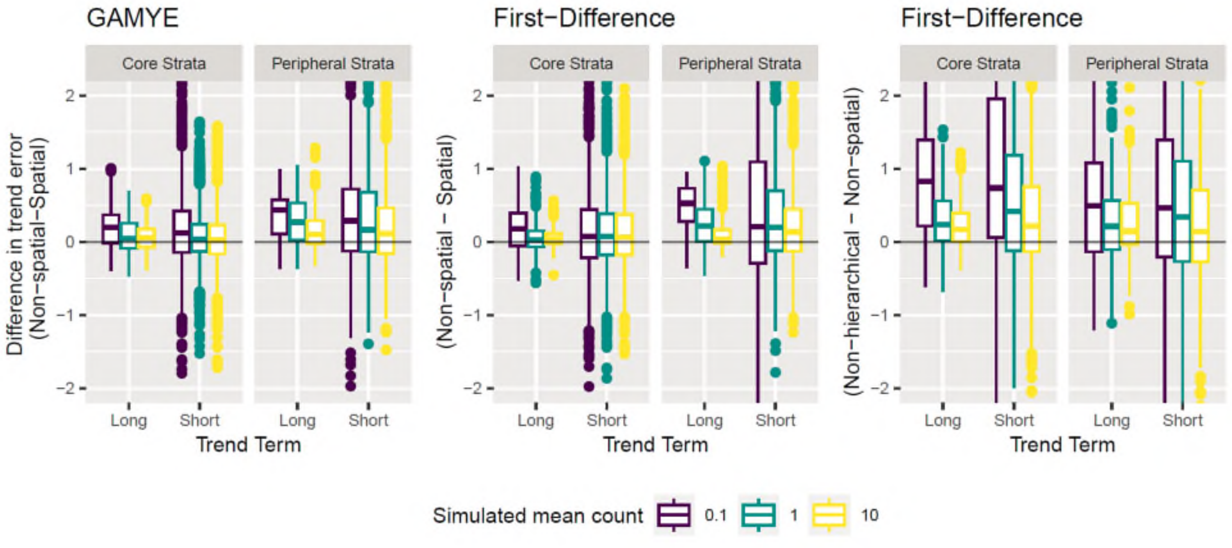

Figure S1. The difference in absolute error of trend estimates between spatial and non-spatial versions of the GAMYE and first difference models for the simulated data (left and center plots) and between the non-spatial and non-hierarchical versions of the first difference model (right plot). The box and whisker plots represent the distribution of percent/year differences in absolute error (non-spatial – spatial, and non-hierarchical – non-spatial) for trends in each stratum and each length of time (long-term and short-term), so that positive values indicate the spatial model estimates were more accurate than the non-spatial models and the non-spatial model was more accurate than the non-hierarchical (lower error). The colours represent different mean counts of the simulated data (0.1, 1, and 10 birds per survey).

We also fit the non-hierarchical first-difference model to the Eastern Whip-poor-will data from the BBS, and compared estimates to those from the spatial and non-spatial versions of the same model. The overall population trajectory and spatial patterns in the trend estimates varied more between the non-hierarchical and other versions than it did between the spatial and non-spatial. In general, the non-hierarchical population trajectory was smoother overall, spatial patterns in the trends were less clear, and trends in the periphery of the species range more often suggested a stable population (Figure S2). In addition, we compared the absolute value of the trends in each stratum for the same short-term time periods to the number of routes with data in each stratum. This comparison demonstrates that the non-hierarchical version of the model tends to shrink trends towards 0 (i.e., stable) when the data are relatively sparse (Smith and Edwards 2020). This bias towards estimating a stable population is much reduced in either of the hierarchical versions of the model and particularly in the spatial version, where estimates for data-sparse regions of the species’ range can be partly informed by information from the rest of the species’ range (non-spatial models) or from neighboring strata (spatial models, Figure S3).

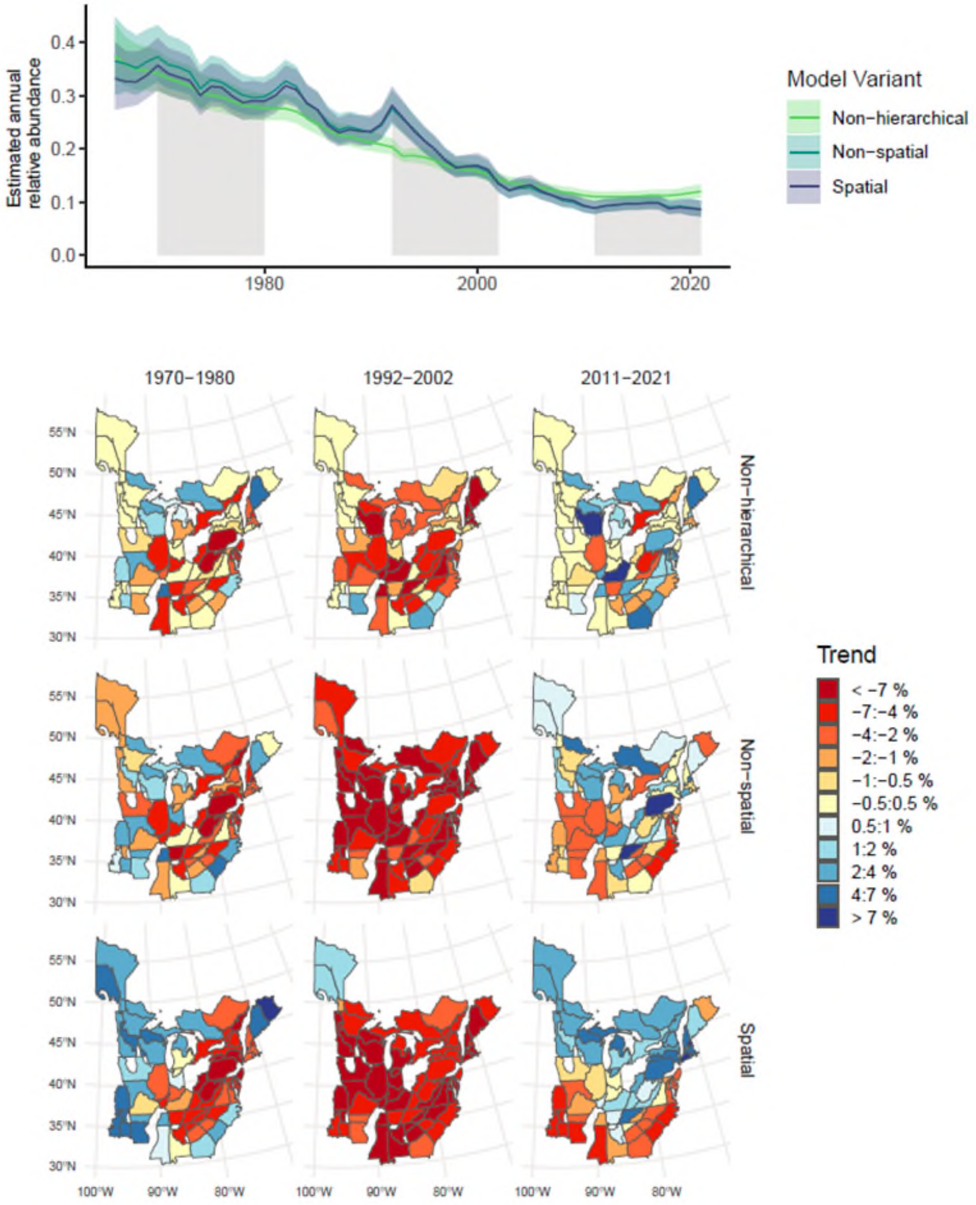

Figure S2. Estimated survey-wide population trajectories and spatial patterns in trends for Eastern Whip-poor-will from the North American Breeding Bird Survey (BBS) from spatial, non-spatial, and non-hierarchical versions of the first-difference model. The trend maps for selected 10-year trend periods highlight the spatial patterns in trends that are evident from the spatial version of the model, somewhat less obvious in the non-spatial version, and largely absent from the non-hierarchical version. The non-hierarchical maps suggest that populations in many strata are relatively stable (lightest colors in the legend). The overall population trajectories are very similar between the spatial and non-spatial versions, but much smoother than in the non-hierarchical version. In addition, the non-hierarchical version suggests a relatively stable population in the most recent period, while the spatial and non-spatial versions suggest a continuing decline.

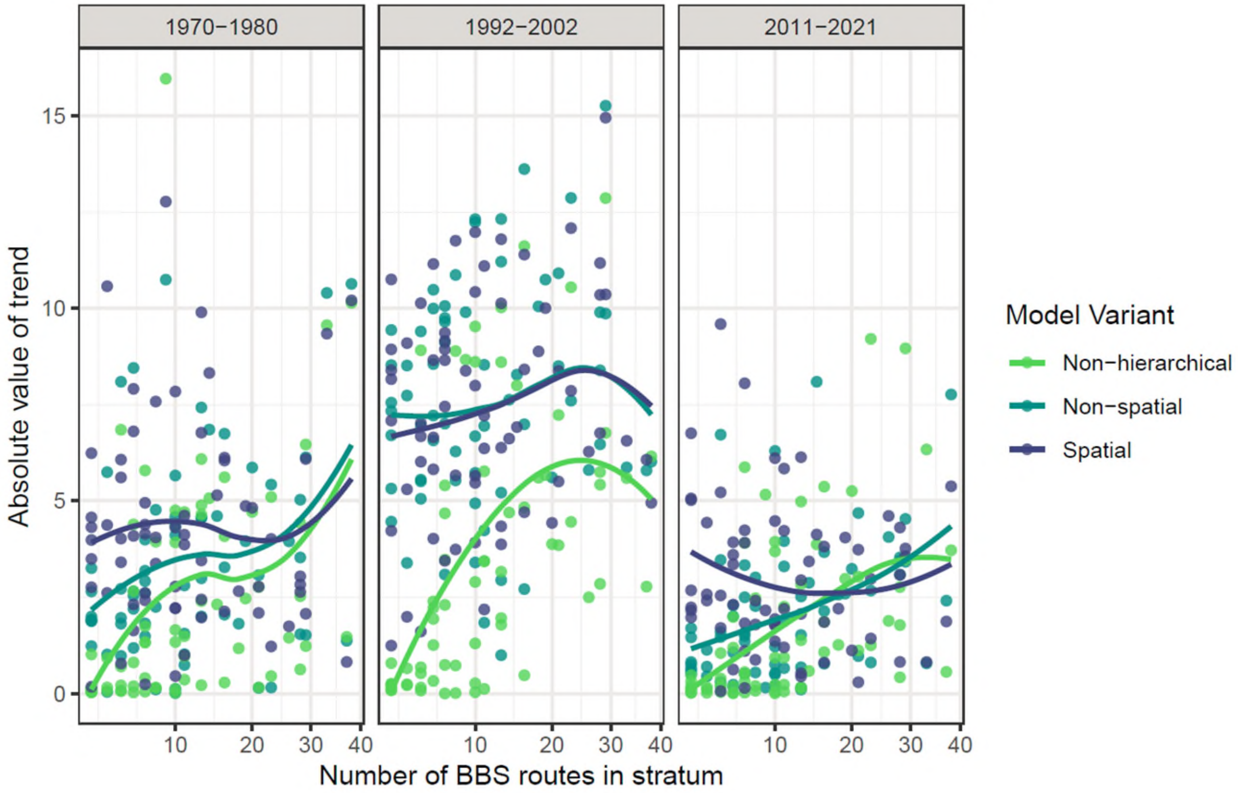

Figure S3. Relationships between the absolute value of estimated stratum-level population trends and the number of BBS routes in each stratum, for three versions of the first-difference model and for three time-periods (the same time-periods visualized in Figure S2) using data from the BBS for Eastern Whip-poor-will. The colored lines represent loess smooths fit to each model’s trend estimates. Estimates from the non-hierarchical version of the model are more likely to be close to 0 (i.e., suggesting a stable population) for data-sparse strata with few routes. The non-spatial model estimates have a much weaker relationship with the number of routes, and the spatial model trends show little or no relationship with the number of routes.

Additional supplemental figures

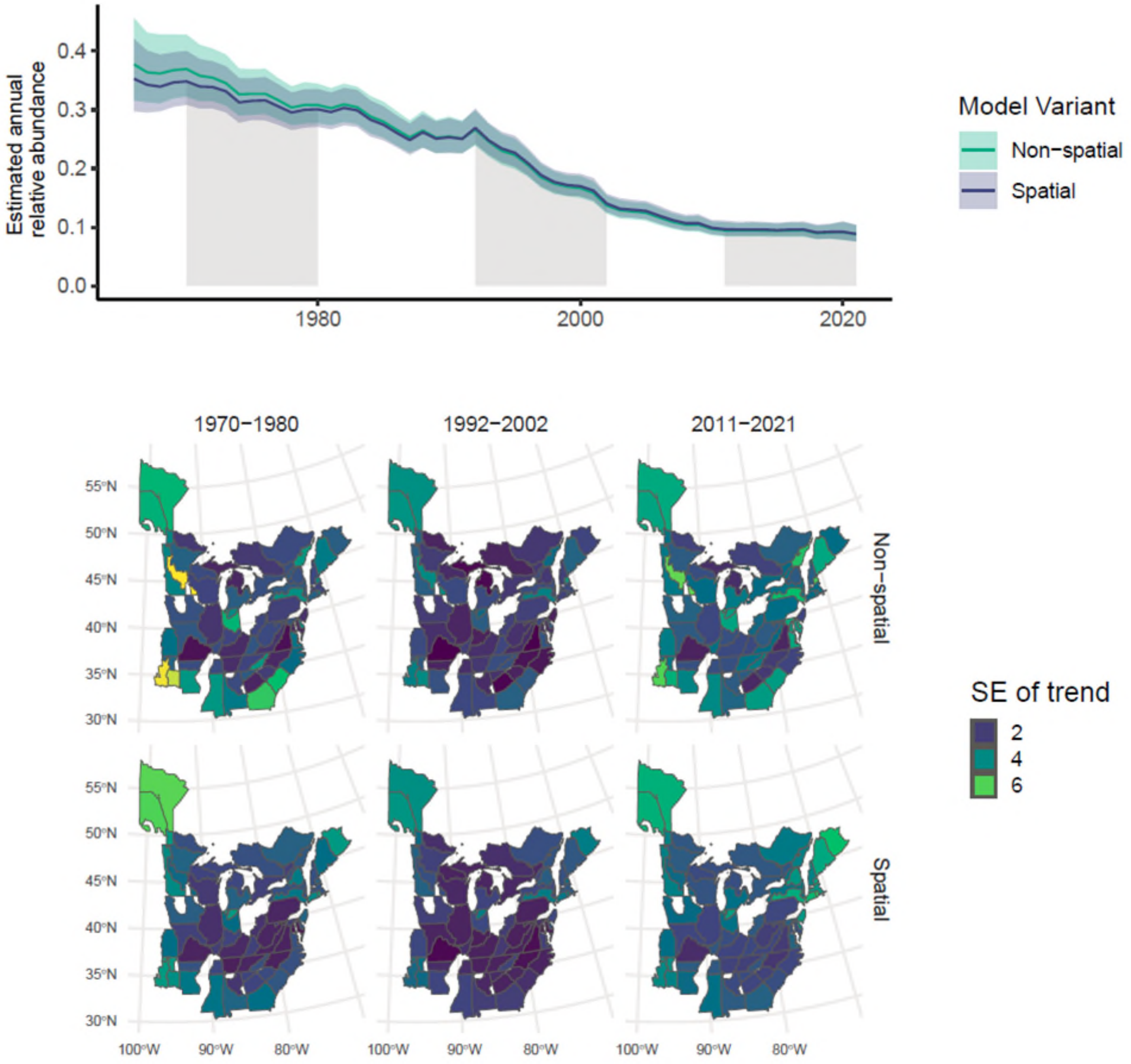

Figure S4. Spatial distribution of trend uncertainty (standard error, SE) for Eastern Whip-poor-will from the BBS data comparing a spatial and non-spatial model. Estimated survey-wide population trajectories and spatial patterns in trend uncertainty for Eastern Whip-poor-will from the North American Breeding Bird Survey (BBS) from spatial and non-spatial versions of the GAMYE model. The trend maps for selected 10-year trend periods highlight the spatial pattern in the uncertainty of trend estimates. In general, standard errors of trends are similar between the two models, but tend to be slightly larger in peripheral strata in the non-spatial version.

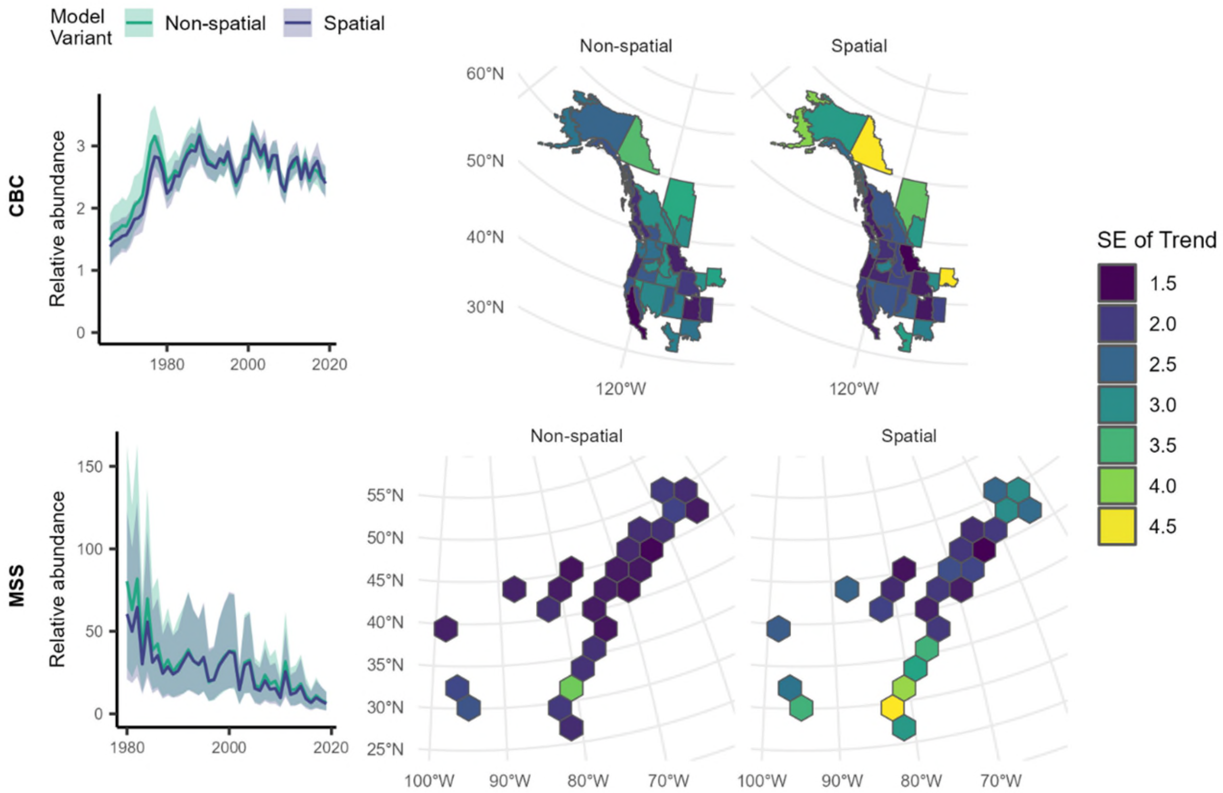

Figure S5. Spatial distribution of trend uncertainty (standard error, SE) for American Dipper and Red Knot using data from the CBC and MSS respectively. Estimated long-term, survey-wide population trajectories and maps of the standard error of long-term trend estimates derived from non-spatial and spatial versions of the GAMYE model. The uncertainties of the overall population trajectories are relatively similar for the spatial and non-spatial models. The maps demonstrate that the spatial models in these two cases tend to have slightly higher uncertainty in some strata especially for the MSS data.

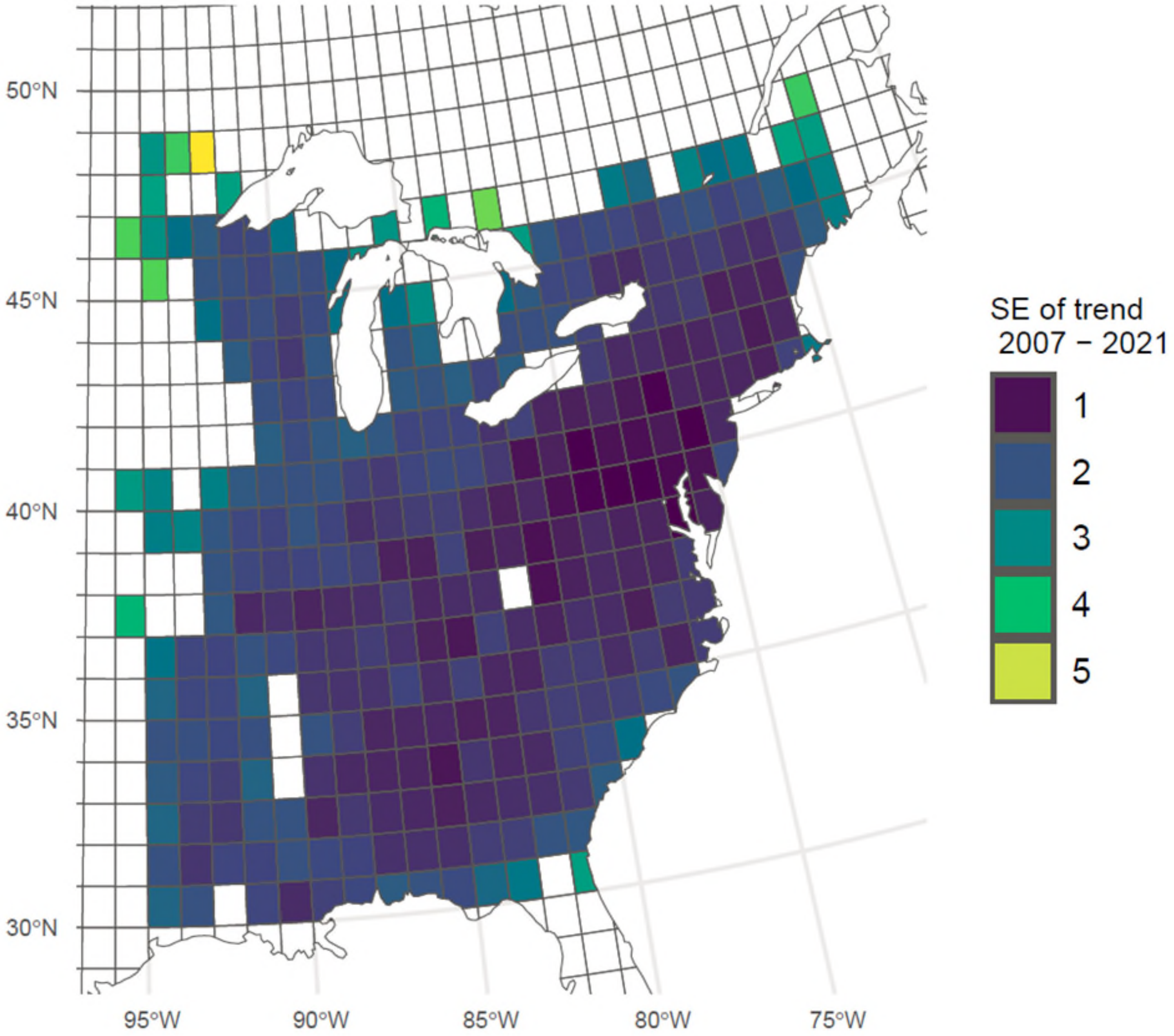

Figure S6. The standard error (SE) of fine-scale trends for Wood Thrush produced by the spatial first-difference model using BBS data (Trends in Figure 6).

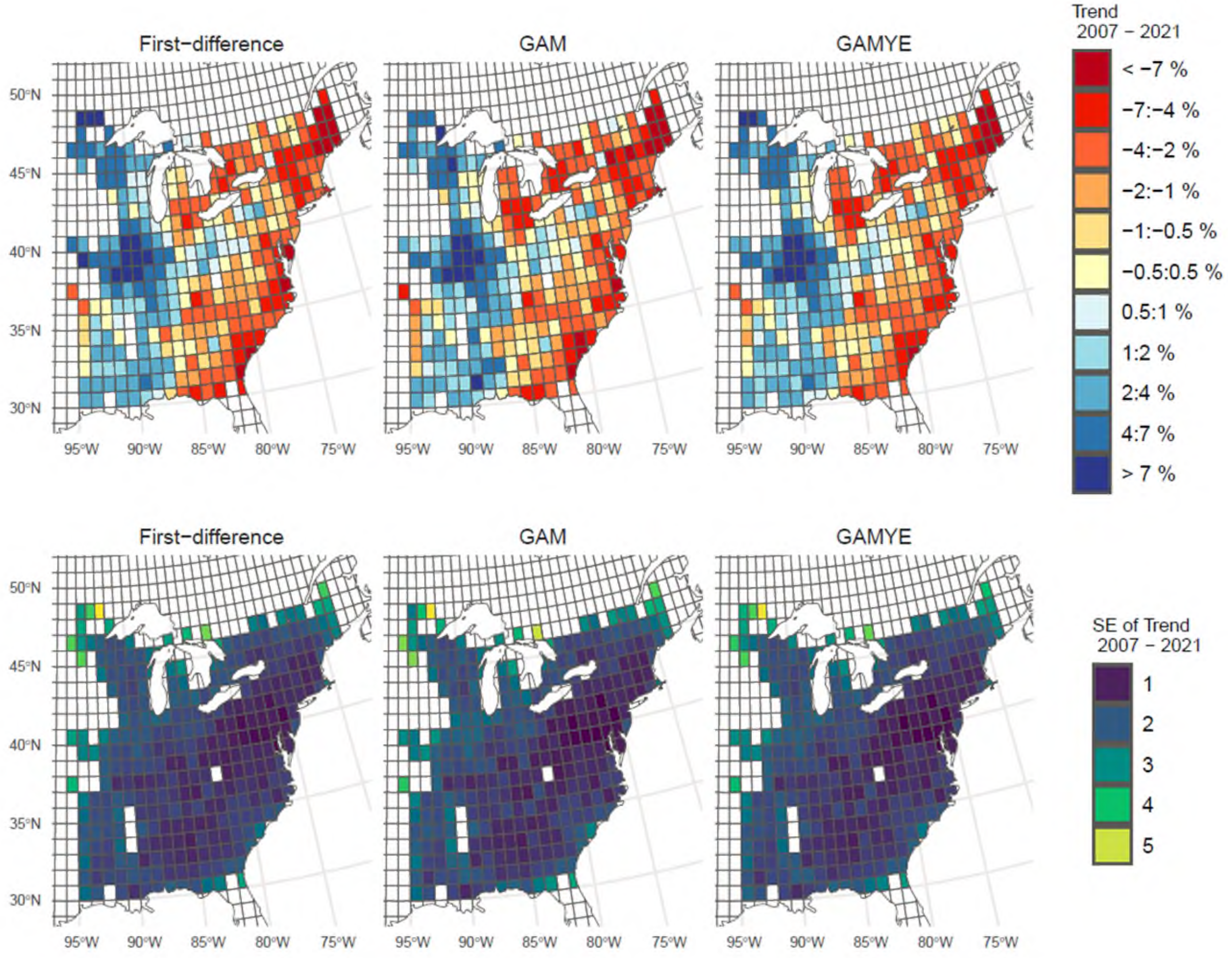

Figure S7. Estimated population trends and standard error (SE) for Wood Thrush from 2007-2021, from spatial versions of the first difference, GAM and GAMYE models applied to BBS data stratified based on a 1 degree latitude by 1 degree longitude grid cells.

Priors and Prior simulation results

Priors

Priors for standard deviations (σ) were generally weakly informative, half standard t-distributions with 3 degrees of freedom (e.g., $\sigma_{\theta} \sim \|t(3,0,1)\|$), which encompass the range of plausible values given the log-scale models. However, some priors on the standard deviations were set to provide a regularizing effect to help constrain the parameters to reasonable values when the data were sparse. For example, we set the priors for the standard deviations of the among observer variation in the BBS model so that 95% of the prior mass was < 1.0 ($\sigma_{\omega} \sim |normal(0,0.3)|$). This somewhat informative prior is reasonable in that it suggests that more than a 2-fold variation in mean counts among observers is relatively rare (i.e., 95% of observers mean counts will fall somewhere between half as many and twice as many birds as an average observer, all else being equal).

We used a prior simulation to establish weakly informative and meaningful priors for the scale of the spline coefficients in the GAMYE ($\sigma_{B'_i}$ and $\sigma_{B''_i}$) and the annual difference parameters in the first-difference models ($\sigma_{\pi'_i}$ and $\sigma_{\pi''_i}$).

Prior Simulation of parameters that control the population trajectories in spatial status and trend models

Our overall goal was to demonstrate some weakly informative priors for the status and trend models based on the realised trend estimates from >50 years of monitoring data from two North American bird monitoring programs, the North American Breeding Bird Survey (BBS) and the Christmas Bird Count (CBC). Conceptually, our goal is to define priors for population status and trend models that reflect our current knowledge about the rates of change and variation in rates of change for bird populations in North America. For omnibus models applied to multi-species surveys like the CBC, BBS, and Shorebird migration monitoring, we suggest that priors with a weak regularizing effect are preferable to priors that imply more temporal and spatial variation.

1. The weakly informative and mildly regularising priors reflect two explicit assumptions:
   that rates of population change and variation in those rates for any given species are very likely to fall somewhere within the range of comparable parameter estimates for past data from all of the other species in similar monitoring programs.
2. That extreme trends and extreme levels of variation in trends are unlikely without evidence to support those extreme values.

These simulations demonstrate the distribution of predictions from these models when there are no data. Given the broad spatial and temporal scale of these monitoring programs and the 1000s - 100,000s of observations for any given species, these priors are primarily relevant in the most data-sparse regions or time-periods for any given species.

Methods overview

Using the published annual indices of relative abundance (i.e., the population trajectories) published by the USGS and Audubon, we can generate reasonable estimates of the realised distributions for some key population parameters for North American birds. Together, these two programs estimate population trajectories and trends for > 600 species of birds. Using these population trajectories we estimated trends in populations at two spatial scales: province/state and survey-wide. We estimated the spatial variation in the trends by estimating the standard deviation of province/state trends within species. We estimated these trends and spatial variation in trends for a range of temporal scales, including 1-year annual fluctuations, short-term trends, and long-term trends.

We then compared prior predictions of trends from our status and trend models with the realised distributions of trends and variation in trends. These comparisons allow us to choose weakly informative priors for the status and trend models that are sufficiently flexible to cover most of the observed variation in trajectories without including significant prior probability for implausible rates of population change or regional variations in those rates. Specifically, we use these simulations to set priors on the spline parameters and annual fluctuations in the GAMYE, annual differences in the first-difference model, and the variation among regions in these same parameters (both spatially explicit and non-spatial versions).

Simulation summary

For both the spatial and non-spatial GAMYE models, we used the following priors for the hyperparameters that control the mean overall smooth and the year-effects (random annual fluctuations around the smooth) within each stratum:

- standard deviation of the spline parameters that govern the shape and flexibility of the overall mean smooth = $\sigma_{B'_i} \sim |t(3, 0, 1)|$.
- standard deviation of the year-effects in a given stratum = $\sigma_{\gamma_i} \sim Gamma(2, 10)$. This is a boundary avoiding prior that puts 95% of the prior mass at values less than 0.5, annual fluctuations greater than ~50% are unlikely, but the long tail allows for much larger values when supported by the data.

For the spatial GAMYE, to control the variation in the shape of the smooth component of the population trajectory in each region:

- standard deviation for a given knot in the basis function controlling the variation among regions = $\sigma_{B''_i} \sim |normal(0, 1)|$.

For the non-spatial GAMYE, to control the variation in the shape of the smooth component of the population trajectory in each region:

- standard deviation of the collection of spline parameters in each region = $\sigma_{B''_i} \sim |normal(0, 1)|$.

For the spatial and non-spatial first difference models, the standard deviation of the differences between subsequent years control the shape of the population trajectory. We used the same priors in these two models:

- standard deviation of the differences between years in the overall mean population trajectory = $\sigma_{\pi'_i} \sim |t(3, 0, 0.1)|$. This prior suggests that it is unlikely that the average annual changes in the survey-wide (continental) population would be greater than 20%.
- standard deviation of the among strata variation in the annual change in populations = $\sigma_{\pi''_i} \sim |normal(3, 0, 0.2)|$. This prior suggests that it is unlikely that the average among strata variation in annual population change would be greater than 40%.

For the non-hierarchical first difference model, population trajectories are estimated independently in each stratum, and there is no mean overall trajectory. In this model only one parameter controls the shape of the population trajectory in a given stratum:

- standard deviation of the differences between years in the population trajectory = $\sigma_{\pi_i''} \sim |normal(3, 0, 0.2)|$. This prior suggests that it is unlikely that the average annual changes in the stratum-level population would be greater than 40%.

These plots show the frequency distribution of prior predictions from the various models in coloured lines against the distribution of realised trend estimates from all species in both the BBS and CBC datasets, for all possible 1-year, 10-year, and 50-year periods in the datasets 1966-2019. To simplify the displays and to account for any bias in the direction of the realised trends from the BBS and CBC, we converted all trends (prior predictions and realised values) to their absolute values.

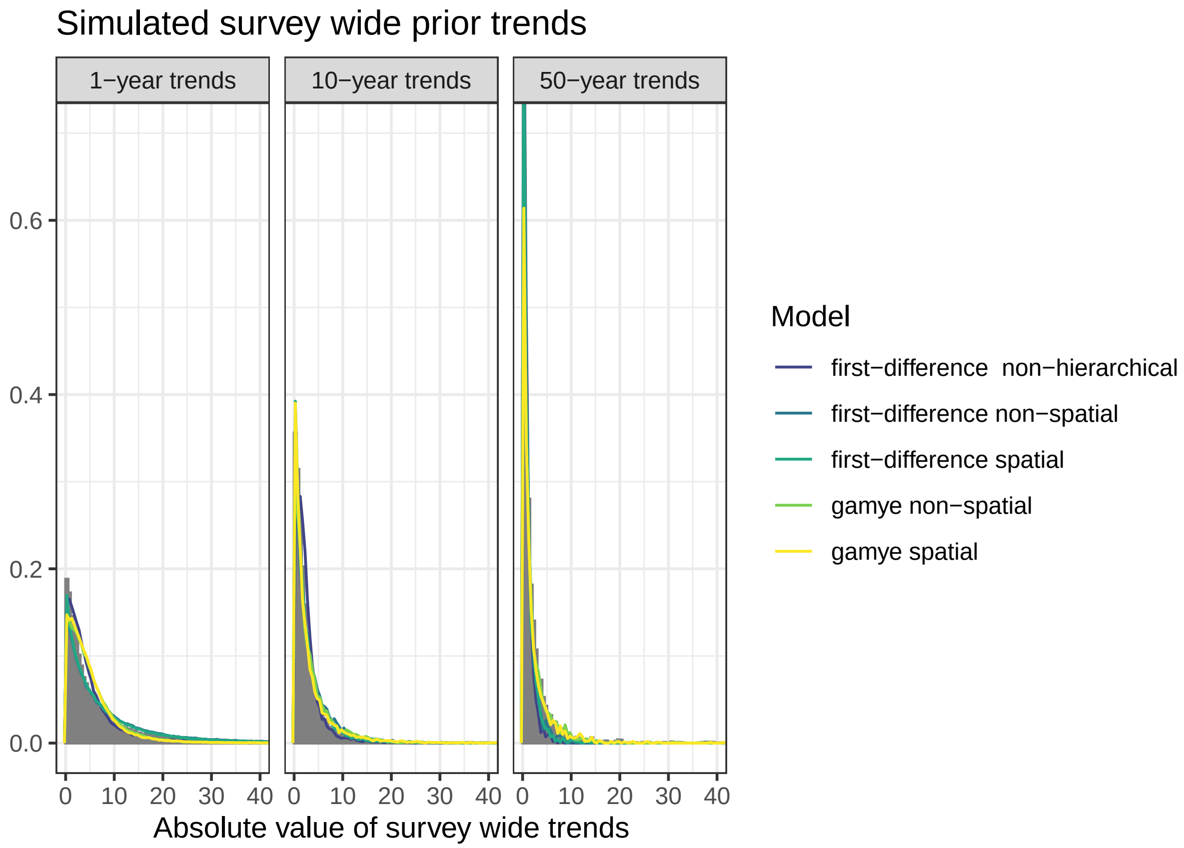

The prior predictive distributions of the absolute value of survey-wide trends align closely with the realised distribution of absolute values of survey-wide trends for various time-scales.

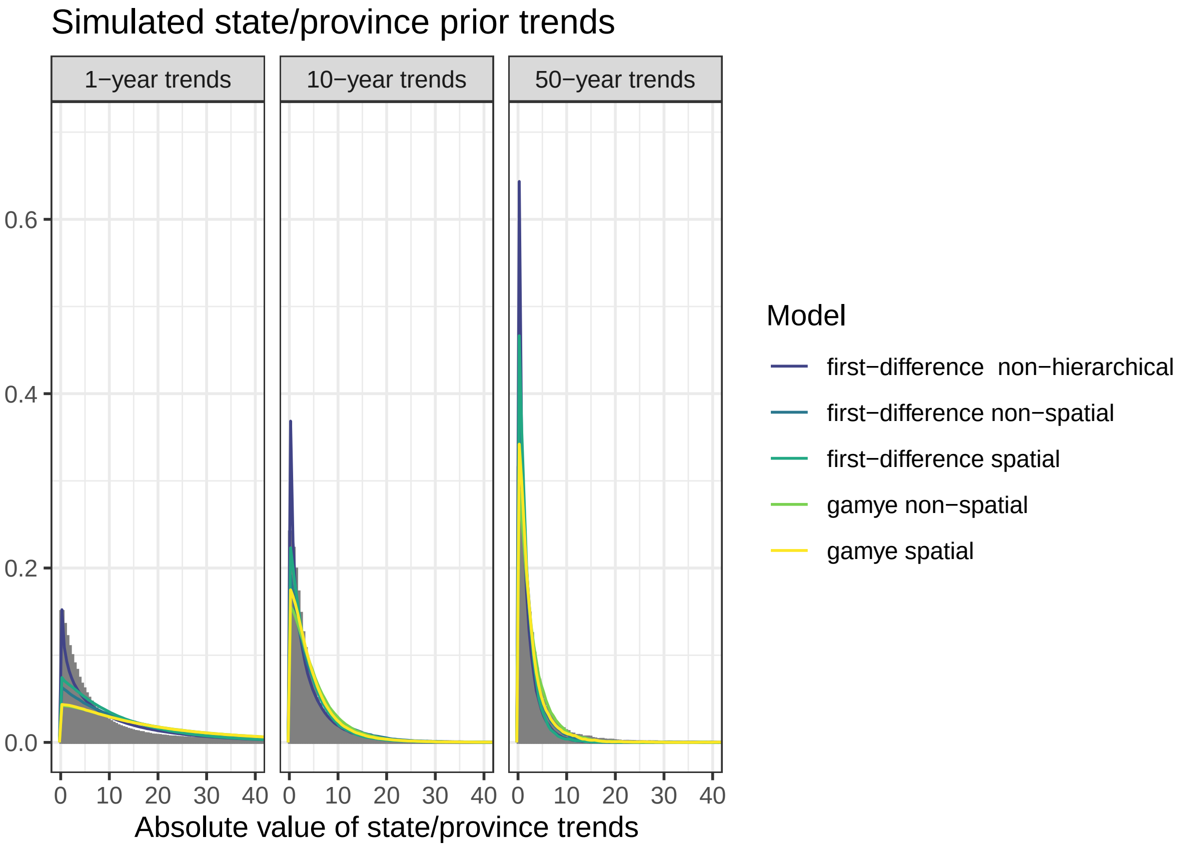

The prior distributions of the absolute values of strata-level trends also align well with the realised trends. The prior predictions for GAMYE models fit best for the 10 and 50-year trends and tend to suggest much more variation in the short-term. Arguably, the priors for the scale of the year-effects may be too wide, because 1-year trends from the GAMYE generally include large amounts of prior mass at values greater than those commonly observed in the realised data. By contrast, the first difference predictions align most closely with the 1-year trends and suggest that extreme values of long-term trends are less probable.

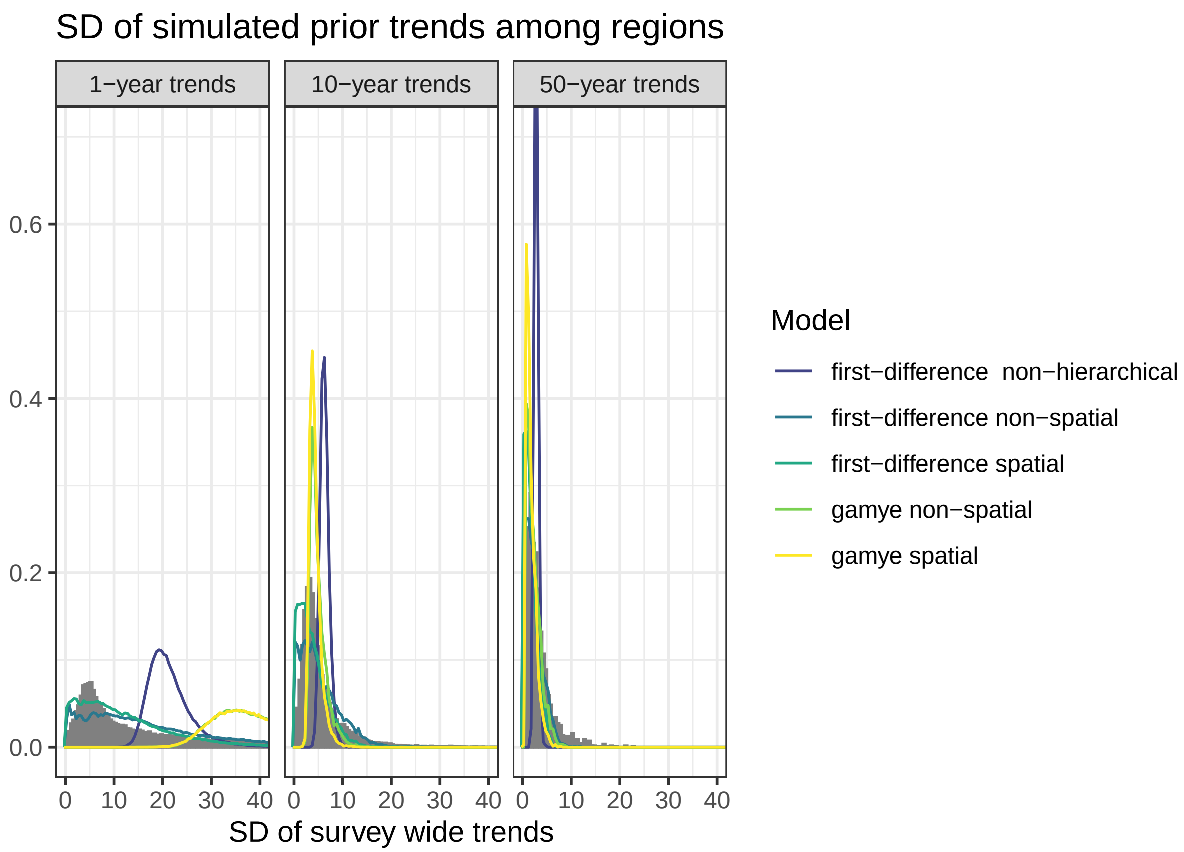

The prior distributions of the standard deviation of trends among regions are more complicated. These priors vary among the lengths of the trends and the models. We selected our priors to balance between implying too much variation in the short-term trends and a regularizing effect on the variation in the long-term trends. The first-difference priors for the spatial and non-spatial models align well with the realised distribution of the 1-year trends, and also provide some regularisation on the variation in long-term trends. By contrast, the independent estimation of trends among regions in the non-hierarchical version of the first-difference model suggests greater variance in 1-year trends and a much narrower range of variation in long-term trend variation, than is observed in the realised data. For the GAMYE models, the variation in the 1-year trends is greatly over estimated, due to the influence of the random annual fluctuations that vary independently among strata. These priors also have a similar regularizing influence on the variation in long-term trends.

We suggest that this regularizing effect on the variation in long-term trends is desirable.

- These are only priors, and so with data to support greater variation among regions, the model predictions will support that greater variation.
- Without a regularizing influence from the model, sampling error in data-sparse regions can lead to apparently extreme trend estimates that may have an undesirable effect on the composite survey-wide trend estimates.
- The regularizing effect on long-term trends still includes some very extreme levels of variation. For example, most of the priors here suggest that standard deviations in trends among regions are unlikely to be $>$ 6-7%/year. This level of variation among regions in a 50-year trend implies that on-average, a species with an overall stable population will include regions that have 50-year trends of +7%/year and have therefore increased by more than 2000%, and regions that have -7%/year trends and have therefore decreased by 97%.